



**NTNU – Trondheim**  
Norwegian University of  
Science and Technology

# Line-Of-Sight-based maneuvering control design, implementation, and experimental testing for the model ship C/S Enterprise I.

**Nam Dinh Tran**

Marine Technology

Submission date: June 2014

Supervisor: Roger Skjetne, IMT

Co-supervisor: Øivind Kjerstad, IMT

Norwegian University of Science and Technology  
Department of Marine Technology





## PROJECT DESCRIPTION SHEET

<b>Name of the candidate:</b>	Dinh Nam Tran
<b>Field of study:</b>	Marine control engineering.
<b>Thesis title (Norwegian):</b>	Design av regulatoralgoritme for banefølgning ved siktlinjemetoden, implementering, og eksperimentell testing for modellfartøyet C/S Enterprise I.
<b>Thesis title (English):</b>	Line-Of-Sight-based maneuvering control design, implementation, and experimental testing for the model ship C/S Enterprise I.

### Background

The maneuvering control problem was defined in 2002, providing a novel framework for solving path-following problems for a wide variety of dynamical systems. By dividing the overall maneuvering problem into a geometric and dynamic task, the methodology provides means to construct intelligent control and guidance laws with natural behavior in terms of how a dynamical system solves a path-following control objective. Within the field of marine technology, several applications have been reported in the literature, including pipe-laying operations, transit operations, and cooperative formation control for groups of surface vessels.

Recent developments have resulted in a generalization of the original maneuvering problem. Instead of focusing solely on one-dimensional paths, the objective is to ensure that the output of the controlled system converges to any desired manifold. This extension provides greater flexibility, effectively extending the possible applications of the design methodology. Although several applications already have been documented for marine vessels such as formation control, Line-Of-Sight (LOS)-based guidance and control, and extensions of maneuvering-based path-following with positional constraints, few experiments have yet been conducted. The aim of this thesis is therefore to design a LOS-based maneuvering control law for the model ship C/S Enterprise I (CSE1), implement this on its real-time control system architecture, and test it in the Marine Cybernetics Laboratory (MC Lab).

### Work description

1. Allocate time in MC Lab for experimental testing.
2. Describe the new modularized HW/SW architecture for CSE1. This should show how different control modes for CSE1 is implemented in separate modules and how one can switch between these control modes. The description should explain the main function(s) of each control mode and what resources that are required (e.g. what measurements must be available, communication, etc.)
3. Perform a (literature) study on applications of CSE1 in projects and papers, on the maneuvering control design method, and on LOS-based control designs. Write a list with definitions and descriptions of relevant terms and concepts.
4. Let  $p = (x, y)$  be the position of a point mass, with a double integrator dynamics, i.e.  $\ddot{p} = u$ . Let a desired path be a straight line, to be traversed with unit speed. Implement and simulate a maneuvering control law for this system and explain its behavior in terms of how and why the filtered/unfiltered gradient update laws work.
5. Propose how to implement a LOS-based maneuvering control mode within the control system architecture for CSE1, with functionalities for setting the path, specifying the speed along the path, and to get feedback on the actual motion of the ship relative to the desired path in the lab.
6. Design a guidance system and a LOS-based maneuvering control law based on full actuation of CSE1. The path given by the guidance system should utilize the space in MC Lab as much as possible without needing to terminate early the operation due to space constraints. To consider if one can move the carriage during experiments to get more space available. Present simulation results for the system.

7. Implement and test the LOS-based maneuvering control system for CSE1 in MC Lab and present the experimental results.

**Tentative:**

8. Design, implement, and test an underactuated LOS maneuvering control law for CSE1.

**Guidelines**

The scope of work may prove to be larger than initially anticipated. By the approval from the supervisor, described topics may be deleted or reduced in extent without consequences with regard to grading.

The candidate shall present his personal contribution to the resolution of problems within the scope of work. Theories and conclusions should be based on mathematical derivations and logic reasoning identifying the various steps in the deduction.

The report shall be organized in a rational manner to give a clear exposition of results, assessments, and conclusions. The text should be brief and to the point, with a clear language. The report shall be written in English (preferably US) and contain the following elements: Abstract, acknowledgements, table of contents, main body, conclusions with recommendations for further work, list of symbols and acronyms, references, and (optionally) appendices. All figures, tables, and equations shall be numerated. The original contribution of the candidate and material taken from other sources shall be clearly identified. Work from other sources shall be properly acknowledged using quotations and a Harvard citation style (e.g. *natbib* Latex package). The work is expected to be conducted in an honest and ethical manner, without any sort of plagiarism and misconduct. Such practice is taken very seriously by the university and will have consequences. NTNU can use the results freely in research and teaching by proper referencing, unless otherwise agreed upon.

The thesis shall be submitted with two printed and electronic copies, to 1) the main supervisor and 2) the external examiner, each copy signed by the candidate. The final revised version of this thesis description must be included. The report must appear in a bound volume or a binder according to the NTNU standard template. Computer code and a PDF version of the report shall be included electronically.

**Start date:** August, 2013                      **Due date:** As specified by the administration.

**Supervisor:** Roger Skjetne  
**Co-advisor(s):** Øivind K. Kjerstad (PhD candidate)

**Trondheim,**

---

**Roger Skjetne**  
Supervisor

# Summary

This report documents the progress, methods and engineering in building and testing the framework for CyberShip Enterprise 1. The main focus have been to modularize, standardize and improve the infrastructure and the operative system with respect to performance. With a secondary objective to create a user-manual to operate it.

The work is done for a surface vessel in 3 degrees of freedom, surge, sway and yaw, and in calm waters and slow speed.

The reliability when conducting laboratory experiments with CyberShip Enterprise 1 have greatly improved. This was achieved through repositioning and replacing the antenna for wireless communication, and a restructuring of how signals were handled between servers and softwares. The original setup with single frequency was replaced with a multi-frequency producer-consumer structure.

The futherst away a vessel is visible for Qualinsys is around 17 meters from the cameras. The shortest distance is roughly 4 meters infront of the cameras. This result in a lengthwise workspace for a vessel to be in the range of 13 meters. This length length can be increased to 27 meters, If the carriage start from the beach end, and moves toward the wavemaker during the experiment. It is not possible to increase it futher due to the length of the basin, the wavemaker, beach, in/outlet and carriage is occupying.

In the system identification, an addtitional hydrodynamic damping coefficient for slow speed have been determined for the hull ( $N_v = 0.18140$ ). In addtion higher order coefficient have also been estimated from the towing measurements. A pseudo library for lookup table thruster mapping have been created. The bow thruster have been mapped for power limit input =  $\{0.15, 0.3, 0.4, 0.5\}$ , and the voith schneider propellers for speed input =  $\{0.3, 0.4\}$ . Measurments for voith schneider propellers for speed = 0.2 have also been conducted, but no lookup table have been created for it.

The starboard voith schneider propeller rotates slow than the port voith schneider propeller. It is also noted that the servos are significantly coupled and the force output drops at the periphery value , 1 . Of the servos, servo 4 have the strongest coupling in surge-sway.

Two advance control design were implemeted, tuned and tested, a *LgV backstepping* and a *Nonlinear PID* designed controller. In the ideal simulated word both of them were equal in terms of maneuvering. Only ellipse path was used in the laboratory. This had to do with space constraints, and a wish to have long run time on the experiments.

Originally only the *LgV backstepping* was tested in the laboratory. It converged and performed well. The only downside was it would constantly overshoot the heading, resulting

in a constant oscillation, while moving along the path. The reason was due to the noisy velocity estimation.

In the laboratory, their performance depended heavily on how they were implemented. If both of them were fully implemented, *LgV backstepping* proved to handle the uncertainties better. Although it would overshoot when exiting the sharper part of the ellipse path. While the fully implemented *Nonlinear PID* would struggle to converge to the path and behave erratic. The velocity dependent term distorted *Nonlinear PID*'s results the most.

The *Nonlinear PID* is the superior one if only the first term is active. It would converge naturally to the desired position. Once on, it would stay there indefinitely despite of the broken servo arm.

With all the improvement in the reliability, one important problem still remains; the loss of visibility. There are incidents when Qualinsys displays it sees all marks, but it is unable to calculate the vessels position and orientation. The cause of this needs to be further investigated. Spare part servo arms should be purchased, and padding for the hull to dampen the impact to the basin walls. Several cracks have been observed on the hull. Simulation Interface Toolkit have been discontinued, modifying it for Modular Interface Toolkit can be an option. The labeling and choice of variable name can be improved upon.

# Preface

This thesis concludes my M.Sc studies, not what I expected, but more than what I could hope for. The purpose of this report was to document the work carried out in the Marine Cybernetics Laboratory at the Norwegian University of Science and Technology since Fall 2013. The original version of this report and content was lost durring transit as a result of several unfortunate decisions. What is presented here is a shell of the original, recreated during the last two weekends before the deadline. In hinsight, hubris was the reason, as they say, *pride come before the fall*.

The work began with reviewing the previous work done on CyberShip Enterprise 1, before restructuring and improve it. This lead to a more modularized and generic control architecture suitable for many types of control designs. In relation to this work, countless days have been spent in the Marine Cybernetics Laboratory conducting measurements of various parameters related to controlling CyberShip Enterprise 1.

This report tries to cover the main points of the original, an overview of the infrastructure used by CyberShip Enterprise 1, the work related to it, and laboratory experiment carried out with it.

I want to first and foremost thank my supervisor Roger Skjetne, for his advice, knowledge and suggetions. Without those the final control architecture would be a real mess to work with. And also for the opportunity to with CyberShip Enterprise 1.

I would like to thank my co-advisor Øivind K. Kjerstad for his inputs and support throughout this endeavor, expecially durring the the frustrating periods of debugging. I would also like to express my graditude to Senior Engineer Torgeir Wahl for his assistance when working in the laboratory, for teaching me how to utilize the various equipments, and for developing the software need to improve the overall reliability. Lastly a thanks to my family for nugging me in this direction.

Looking back, working on this (pre-report writing) have been the highlight of my life up to this point. I have learned more the last year than any of the previous ones.





# Contents

<b>Project description</b>	<b>i</b>
<b>Summary</b>	<b>iii</b>
<b>Preface</b>	<b>v</b>
<b>1 Introduction</b>	<b>1</b>
1.1 Motivation	1
1.2 Background	1
1.3 Previous works	2
1.4 Preliminaries	2
1.4.1 Notations	2
1.4.2 Reference frames	3
1.5 Model	3
1.6 Software	4
1.7 Scope	4
1.8 Structure	5
<b>2 The Infrastructure</b>	<b>7</b>
2.1 Overview	7
2.2 CyberShip Enterprise 1	8
2.2.1 Communication	8
2.2.2 Visibility	9
2.2.3 Thrusters	9
2.3 Marine Cybernetics Laboratory	10
2.4 Qualisys	10
2.5 LabVIEW	10
2.5.1 .vi files	11
2.5.2 Front Panel	12
2.5.3 Block Diagram	13
2.5.4 Simulation interface toolkit	13
2.5.5 Qualisys Track Manager Drivers	14
2.6 Simulink	15
2.6.1 Input from LabVIEW	16
2.6.2 Output to LabVIEW	16
2.6.3 Guidance	16
2.6.4 Control	20

---

2.6.5	Plant	23
2.6.6	Navigation	24
2.6.7	C/S Enterprise 1 Matrices	25
2.6.8	Data logging	25
<b>3</b>	<b>System identification</b>	<b>27</b>
3.1	Hull	28
3.2	Thruster mapping	28
<b>4</b>	<b>Line of Sight Experiments</b>	<b>33</b>
4.1	Simulation runs	33
4.2	Laboratory runs	33
<b>5</b>	<b>Conclusion</b>	<b>35</b>
5.1	Future works	36
	<b>Bibliography</b>	<b>36</b>
	<b>Glossary</b>	<b>39</b>
	<b>Acronyms</b>	<b>41</b>
	<b>Symbols</b>	<b>43</b>
	<b>Appendix</b>	<b>44</b>
<b>A</b>	<b>Thruster plots</b>	<b>45</b>
<b>B</b>	<b>Draft for User Manual</b>	<b>73</b>

# Chapter 1

## Introduction

This chapter provides the general background information to grasp a better understanding of the following chapters. The thesis can be shortly described as a report focusing on the maneuvering of a surface vessel in calm water and slow speed, and the infrastructure surrounding [CyberShip Enterprise 1 \(CSE1\)](#).

### 1.1 Motivation

In the academic world of marine cybernetics, there are many great ideas. However they remain there due to several factors, among others, the amount of resources need to process, refine, simulate and verify them. Those that makes it past those initial stages, often stops on the boarder between the academic and real world. The reasons can be many, one might be limited possibility for real world verification.

Real world experiments are an important part of verifying designs and theories. The cost of doing this in full scale and out in the field can be both a costly and time-consuming investment of resources. A more reaonable, practical and effective way is to perform laboratory experiments, since it is down scaled both in terms of size and cost. It can provide a proof of concept beyond just simulations, and a stepping stone towards a full scale experiment.

This thesis aims to advance one of these great ideas, Line-Of-Sight-based maneuvering control design, and hopefully provide an easy framework for others to work on.

### 1.2 Background

The model based ship control began with the introduction of the gyrocompass in 1908, and was further developed as other positioning systems became available. Another way to look at is the dawn of autopilots. The purpose is to carry out operations or maneuvers without constant human intervention. It can be applied surface and underwater vehicles. Examples of this can be station-keeping, weather optimal positioning and tracking. There are various ways to attain these objective, it can be through a simple [Proportional-Integral-Derivative](#)

(PID)- (linear or nonlinear, with feedback, feedforward, neither, both or just one of them), Linear Quadratic Optimal-, Backstepping-, Sliding Mode-Control and several others. A path can be parameterized discrete, continuous or a hybrid of those, for details on these topics see Skjetne (2005), Fossen (2002) and Fossen (2011)

This thesis will use a continuous path and look at a backstepping- and a nonlinear control with Line-Of-Sight-based maneuvering control design. Another way to describe it is, path-following through forward speed and heading from two different approaches.

## 1.3 Previous works

The maneuvering design approach divides the problem statement into two: a *Geometric Task* and a *Dynamic Task*. The geometric task is to force the output to converge to the desired point or path. While the dynamic task is to force the output to converge to a desired time signal, speed and or acceleration. It was introduced in Skjetne (2005) and more details can be found there and in Fossen (2011).

In Breivik and Fossen (2005), a general framework for path-following is presented, and in Skjetne et al. (2011) the path-following is applied as a generic problem with **Line-Of-Sight (LOS)** and the maneuvering approach. A step further is taken in Thorvaldsen (2011), where he explores the possibility of path-following in formation using different designs, among those the generic maneuvering theory and **LOS** steering algorithm.

**CSE1** have been used in Sundland (2013) for experiments related to towing of icebergs. However several complications made it difficult to produce good results and they are addressed and improved upon in this thesis. **CSE1** was originally developed for demonstrations and experiments at **Marine Cybernetics Laboratory (MC Lab)**, and it is documented in Skåtun (2011). His framework have been deconstructed and reconstructed in preparation for this thesis, see extract of Tran (2013). Instead of quoting half of Skåtun's thesis, it should be read before reading this thesis, as it is the foundation buildt upon. This thesis is a continuation, where it will further develop and elaborate on the mechanics of **CSE1**'s framework.

## 1.4 Preliminaries

### 1.4.1 Notations

The notations corresponds with Skjetne's and Thorvaldsen's work.

Time derivatives of  $x(t)$  are denoted as  $\dot{x}$ ,  $\ddot{x}$ ,  $x^{(3)}$ ,  $\dots$ ,  $x^{(n)}$ , while partial differentiation:  $\alpha^t(x, \theta, t) := \frac{\partial \alpha}{\partial t}$ ,  $\alpha^{x^2}(x, \theta, t) := \frac{\partial^2 \alpha}{\partial x^2}$  and  $\alpha^{\theta^n}(x, \theta, t) := \frac{\partial^n \alpha}{\partial \theta^n}$ . The Euclidean vector norm  $|x| := (x^T x)^{1/2}$  and stacking vectors into one is denoted as  $col(x, y, z) := [x^T, y^T, z^T]^T$ . The subscript  $d$  stand for *desired*.

### 1.4.2 Reference frames

**Q-frame:** is a inertial reference frame within **MC Lab** similar to a North-East-Down frame. It is used by **Qualisys** to determine the position and orientation of the bodies observed. The origin and orientation of the frame is set when calibrating **Qualisys**.

This is done using two sets of **InfraRed (IR)** markers, where in each set the markers have fixed placement relative to eachother. One set of markers is placed on a fixed position, specifying the origin and orientation of the frame, while the other is moved around to calibrate the the the workspace. Normally the x-, y-, and z-axis are parallel the basins walls, where x-axis points toward the wavemaker, y-axis points away from the walkway and z-axis points down.

The orgin is roughly placed along the longitudinal centerline. If the basin is empty when calibrating, the origin is set around approximately half a meter above the basins bottom. If the basin is full when calibrating, then it is set a few centimeters above the water surface. This has to do with the practical aspects of moving, placing and retrieving the markers.

**B-frame:** is a body frame for **CSE1**. The frame moves and rotates with the vessel. The origin is in placed along the longitudinal centerline, approximately on the longitudinal tipping point (determined by balancing **CSE1** on a metal pipe) and on the waterline. The x-axis pointing from stern to bow, y-axis from port to starboard and z-axis top to bottom.

## 1.5 Model

The general model used for **CSE1** to describe the vessel dynamics

$$\dot{\boldsymbol{\eta}} = \mathbf{R}(\psi)\boldsymbol{\nu} \quad (1.1a)$$

$$\mathbf{M}\dot{\boldsymbol{\nu}} = \boldsymbol{\tau} - \mathbf{D}\boldsymbol{\nu} \quad (1.1b)$$

where  $\boldsymbol{\eta} = \text{col}(\mathbf{p}, \psi)$  is the position and heading in the **Q-frame**,  $\mathbf{p} = \text{col}(x, y)$ ,  $\boldsymbol{\nu} = \text{col}(u, v, r)$  is the velocity vector in the **B-frame**,  $\boldsymbol{\tau} = \mathbf{B}\mathbf{f}_{act}$  is the command force vector in **B-frame**,  $\mathbf{R}(\psi)$  is the corresponding  $3 \times 3$  rotation matrix.  $\mathbf{M}$  is the inertia matrix, and  $\mathbf{D}$  accounts for the hydrodynamic damping. See the section about system identification or **Fossen (2002)** for more details.

It is a model suited for ship positioning (**Fossen, 2002**), and is suitable for slow speed and calm water applications. Another reason is due to limited and inaccurate system identification of the hull.

The coefficients in the matrices follows the notion of The Society of Navel Architects and Marine Engineers, **SNAME (1950)**, and are similar to those found in **Skjetne (2005)**.

$$\mathbf{R}(\psi) = \begin{bmatrix} \cos(\psi) & -\sin(\psi) & 0 \\ \sin(\psi) & \cos(\psi) & 0 \\ 0 & 0 & 1 \end{bmatrix} \quad (1.2)$$

The inertia matrix,

$$\mathbf{M} = \begin{bmatrix} m - X_{\dot{u}} & 0 & 0 \\ 0 & m - Y_{\dot{v}} & mx_g - Y_{\dot{r}} \\ 0 & mx_g - N_{\dot{v}} & I_z - N_{\dot{r}} \end{bmatrix}, Y_{\dot{r}} = N_{\dot{v}} \quad (1.3)$$

The hydrodynamic damping matrix,

$$\mathbf{D} = \begin{bmatrix} -X_u & 0 & 0 \\ 0 & -Y_v & -Y_r \\ 0 & -N_v & -N_r \end{bmatrix} \quad (1.4)$$

The thruster configuration matrix is the same as in [Skåtun \(2011\)](#),

$$\mathbf{B} = \begin{bmatrix} 1 & 0 & 1 & 0 & 0 \\ 0 & 1 & 0 & 1 & 1 \\ l_{y1} & l_{x1} & l_{y2} & l_{x2} & l_{x3} \end{bmatrix} \quad (1.5)$$

However the coefficient values have slightly change,  $\mathbf{f}_{act} = \text{col}(f_1, f_2, f_3, f_4, f_5)$  is the force actuator vector, that needs to be mapped to thruster inputs  $\mathbf{u}$ . See the system identification section for details.

## 1.6 Software

The softwares used in this thesis are [LabVIEW 2010 service pack 1](#) with [Field-Programmable Gate Array \(FPGA\)](#), [Real-Time and Simulation Interface Toolkit \(SIT\)](#) module, [MATLAB 2009b](#) with [Simulink](#), [Real-Time Workshop](#) and [Marine Systems Simulator \(MSS\) Guidance, Navigation and Control \(GNC\) Toolbox](#), [Qualisys Track Manager \(QTM\)](#), [BT-Six](#), [PPJoy](#), [MCG Reg 4.0](#), and [TeXworks](#)

[LabVIEW](#) was used to create and is the [Graphical User Interface \(GUI\)](#) to operate [CSE1](#). The [FPGA](#) module is for signal handling within [Compact Realtime Input and Output \(cRIO\)](#). The Real-Time module is for running the programs in realtime. The [SIT](#) module is for connecting [LabVIEW](#) together with [Simulink](#) and [Qualisys](#).

[MATLAB](#) was used for post-processing force ring measurement and generating graphs. [Simulink](#) is used for creating and modifying the control architecture. [Real-Time Workshop](#) is for converging the [Simulink](#) diagram for real-time experiments. Various blocks from [MSS GNC Toolbox](#) are used in the diagram. Simulink version 8.2 have been used for creating some of the pictures found in this report.

[QTM](#) is needed for measuring position and orientation in the [MC Lab](#). [BTSix](#) and [PPJoy](#) are used for signal processing of the [PlayStation \(PS\)](#) controller. [MCG Reg 4.0](#) was used for logging force ring data and [TeXworks](#) for creating this report.

For a simple introduction in how [LabVIEW](#) and [Simulink](#) are connected see [Texas A&M University \(n.d.\)](#)

## 1.7 Scope

As previously mentioned the focus is on surface vessel in calm water and slow speed. This means [3Degrees Of Freedom \(DOF\)](#) surge, sway and yaw, and linear dynamics. This thesis primarily centers around the infrastucture of [CSE1](#), going into detail about the various resources available. Two different approaches are implemeted for path-following within

the control architecture. They are the [LgV backstepping 2 \(LgV2\)](#) and the [Nonlinear PID \(NLPID\)](#) design from [Skjetne \(2014\)](#). The behavior of the controls will be compared to each other. However details of the control designs wont be covered here, just refered to by the equation numbers. Description and comments of the infratructure components, as well as the reason behind them will be documented as far as possible to give a clearer understanding.

It is assumed that the reader have read or have access to [Skjetne \(2014\)](#) and [Skåtun \(2011\)](#). Their contents are omitted, but referred or assumed known to the reader.

## 1.8 Structure

The thesis is structured into five chapters, Introduction, Infrastructure, System identification, Control experiments and Conclusion. The introduction have already been covered.

In the Infrastructure chapter, a general overview is first presented, followed by a description of each component with comments.

The System identification chapter documents the various procedures conducted in the [MC Lab](#) for determining the coefficients of [CSE1](#)'s hull and the thrusters.

In Control experiments, the two controls are presented, analysed and simulated, and the laboratory run results are discussed.

In the last chapter, the main points are summarized, and suggestions for future work are presented based on those.





## Chapter 2

# The Infrastructure

This chapter presents the various components and equipments and how they interact with each other. In the first section, an overview of the infrastructure is presented. The following sections provides a more detailed view of each component of the infrastructure.

### 2.1 Overview

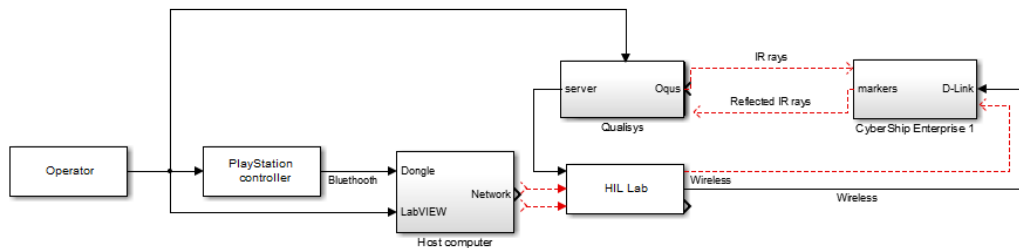


Figure 2.1: General overview of communication.

**CSE1** was buildt with the intension for use in the **MC Lab**. According to [Norwegian University of Science and Technology \(n.d.\)](#), the **MC Lab** was a storage tank for ship models made of paraffin wax and operated by the Department of Marine Technology. It contains a basin with wave-making, towing and real-time position measuring capability. In addition it have equipments for measuring forces and wave heights.

At the time of use, the computers in **MC Lab** were running on Windows XP, limiting the use of software versions to **LabVIEW 2010 Service Pack 1** and **MATLAB 2009b**. As a consequence, the programs developed in this thesis were created for compatability and does not take advantage of certain simpler and more advance functions available in newer versions. The support for Windows XP expired in April 2014, meaning the operating systems needs to be upgraded to Windows 7, lifting the software version restriction.

CSE1 is operated from a laptop using a **LabVIEW Front Panel** as the **GUI**, and the **Block Diagram** and **SIT** for signal routing. The operator have the option of interacting directly with **CSE1** through the **Front Panel** or indirectly through a **PS** controller.

With the indirect approach the **PS** controller communicates with **LabVIEW** via **Bluetooth**. The signals are received by a **Dongle**, and processed first by **BTSix** then by **PPJoy** before **LabVIEW** acquires them. In the current setup, the indirect option have limited applications in terms of control modes. However, this approach can provide a faster, more intuitive and direct control of **CSE1** in terms of manual control. This is due to the mapping which each **Voith Schneider Propellers (VSPs)**'s force direction is mapped to an analog stick, and the lower shoulder button pair (L2 and R2) controls the bow thruster force direction.

The operator also have the option of choosing where the process programs should run, internally (on the laptop) or externally (on the **CSE1**). The former utilize the **.mdl** file while the latter make use of the **nidll\_rtw** files internally and uploads the **nidll\_vxworks\_rtw** files to the **CSE1**. The **nidll\_rtw** and **nidll\_vxworks\_rtw** files are derived from the **.mdl** file using **Real-Time Workshop**. This thesis focus on the latter option. How each signal and controller is treated, is handled and structured in a **Simulink** diagram (**.mdl**).

The communication with **CSE1** occurs wireless through **HIL Lab**. **Qualisys** tracks **CSE1** using **IR** rays and sends the data back to **LabVIEW**.

## 2.2 CyberShip Enterprise 1

In principle **CSE1** consist of a modified hull (1:50 model scale), a waterproof box, a network adapter (D-Link), a **cRIO**, a bow thruster, two batteries, two **VSPs**, four **servos** and several passive **IR** markers, in addition to wires and other electrical components, see **Skåtun (2011)** for details.

### 2.2.1 Communication

Connection between **cRIO** and **LabVIEW** is of the utmost importance, without it, remote control of **CSE1** is impossible. An option to ensure a near 100 % connection is to have a ethernet cable connecting the two together. However, this would severely cripple the mobility, practically mooring it. The other option is wireless connection.

All communication with **CSE1** takes place wirelessly through the D-Link. In the early stages, loss of connection with **CSE1** was a common occurrence. This had to do with where it was relative to where the **HIL Lab** router was and where on the hull the D-Link was placed. Originally the standard antenna was used for the D-Link and placed within the watertight box, bending the antenna almost parallel to the **cRIO**. The combination of these naturally deteriorated strength of the wireless connection.

The loss of connection was lessen with the aid of Senior Engineer Torgeir Wahl. The first action, adding an additional wireless (Asus), placed more centrally and closer to the space **CSE1** operated. However, this solution was short-lived since the Asus died after periode of use. The cause of this is unknown. The next action gave a more permanent fix to the problem. The antenna was moved outside the waterproof box, while the D-Link remained

inside. This was achieved by attaching the D-Link to the inside of the waterproof box's lid with velcro tape, then drill a hole, connect the antenna and sealing it with caulk.

Involuntarily disconnection frequency lessen, but still a nuisance. The last improvement was to replace the standard antenna that followed the D-Link with an antenna roughly three times the original's length. Spontaneous disconnection became more or less extinct. However, it is worth noting that, the probability of establishing connection is mostly determined by the sequence the various wires are connected to the batteries. From experience (without any scientific documentation), connecting the red wire before the black requires fewer attempts of establishing connection than vice versa.

### 2.2.2 Visibility

CSE1's position and orientation are acquired by **Qualisys** using the **IR** markers placed on-board. Therefore size and placement of the markers have an impact on CSE1's visibility. Originally a fixed **IR** marker stand was used and placed on top of the waterproof box along the longitudinal centerline. **Qualisys** had at times and certain orientation relative to the cameras lost sight of CSE1, due to the relative positions of the markers to each other, and their proximity to the latest antenna. Sometimes the markers merge together, other times they overshadow one another, in addition to the antenna overshadowing or dividing the markers.

To increase the visibility, elevated passive **IR** markers were added, two on the longitudinal centerline (bow and stern), three on the aft end (two port one starboard). The first setup had the fixed stand and the five markers, a total of nine markers. With the marker at bow bent forward and the marker at stern bent in the opposite direction. The stand was removed since five markers gives a redundancy of two markers, and the stand could be used for a separate body. The marker at bow was later straighten to be as vertical as possible due to constant shift of its position caused by CSE1 crashing bow first into the basin walls.

### 2.2.3 Thrusters

The thrusters receives control signals from **cRIO**. The bow thruster is a simple tunnel thruster, driven and controlled by a hobby motor. Each **VSP** have a motor for rotation and two **servos** to position the stick. The distance between the stick and **servos** are fixed. However, they move in an circular motion which needs to be accounted for.

## 2.3 Marine Cybernetics Laboratory

The basin's dimensions imposes constraints on the maneuvering space of CSE1. As stated in **Norwegian University of Science and Technology** (n.d.), the basin have a total length of 40 meters, a width of 6.45 meters and it can be filled up to a depth of 1.5 meters. However, measuring it from end to end, it is closer to 39 meters and the length the real length where a vessels position is measurable is limited by several factors.

The basin's water in- and outlet are located at the far end of the basin, as well as its beach. On the opposite is the wave maker. Between those are the measuring equipment, mounted on the front side of the towing carriage. Its motion is limited to the rails along the basin's length, that ends approximately at the edge of the beach. All of this machinery and facility takes up space. The in- and outlet with the beach occupy roughly four meters of the total basin length, around the furthest position the towing carriage can be placed. The towing carriage itself, fills up four meters of length. Lastly the wavemaker takes up about one meter. Using 39 meters as the total length of the basin, a surface vessel should have approximately 30 meters of basin length to maneuver in.

## 2.4 Qualisys

**Qualisys** is the real-time positioning system available in the **MC Lab**. It uses three **IR** cameras (Oqus) to capture the motions. They are mounted on the towing carriage front, one in the middle and one on each side, slightly tilted down.

Oqus sends out **IR** rays which is reflected by passive **IR** markers. If the reflected rays are registered by two or more cameras, and they are able to clearly identify three or more markers, then the position and orientation is captured. The visible field of each Oqus is cone shaped. Due to height placement relative to water surface, the closest visible areas are roughly three meters in front of the cameras. Taking the tilted orientation of the cameras relative to the water surface, size and proximity of the markers the effective range is around 19 meters.

**QTM** is the software that processes the data from Oqus and sends it to a **Qualisys** server, who in turn passes it on to the **HIL Lab** network

## 2.5 LabVIEW

As mentioned previously, **LabVIEW** routes and displays the data. The **Front Panel** provides the **GUI**, and the **Block Diagram** and **SIT** for signal routing. The programs have been deconstructed and reconstructed several times.

The same **.vi**-file can be used for several **.mdl**-files, e.g. "Template HMI.vi" are used for both "TemplateNIPID" files and "TemplateLgV2" files. **SIT** will generate separate project files based on the **.mdl**-file name.

The drivers and **FPGA** files were originally created by Senior Engineer Torgeir Wahl, some of those have later been modified by the author. The programs are intended for single vessel (body), with the possibility to expand for multiple bodies by modifications. The focus will be on single body.

### 2.5.1 .vi files

Four **.vi** files have been created in connection with this thesis, "PS3 HMI.vi", "Thruster HMI.vi", "StudentHMI.vi" and "Template HMI.vi". Each of them shows different stages

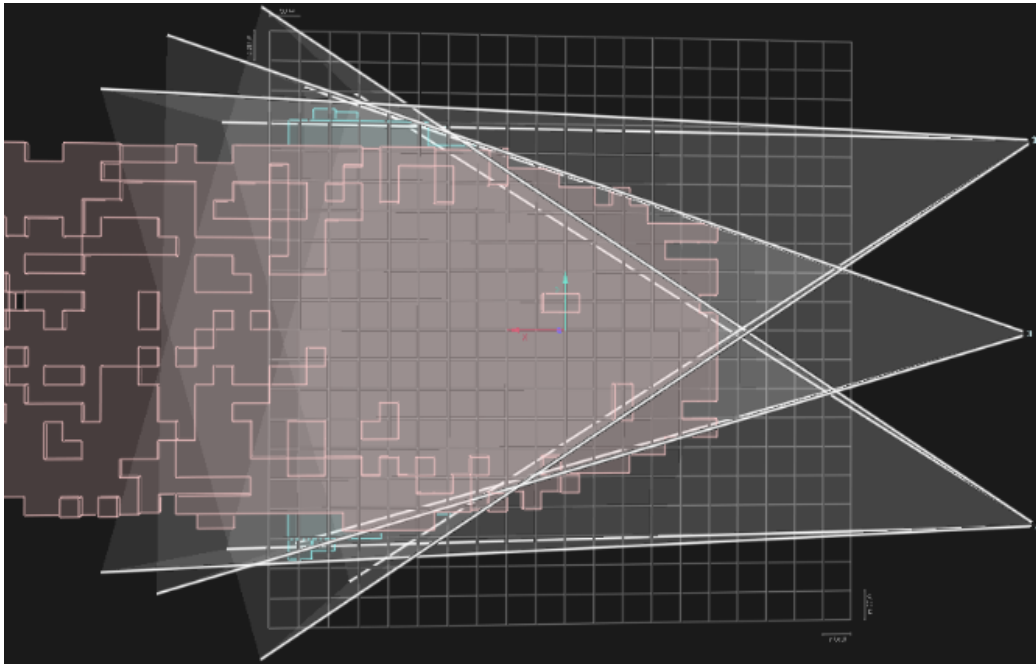


Figure 2.2: Qualisys Oqus area covered seen from above. The Oqus are placed on right edge, white cones indicate visible area per camera. The walkway is at the bottom edge, and somewhere on the left edge is the wavemaker. Red arrow indicate x-axis and teal arrow indicate y-axis. Each square in the grid is  $0.5 \times 0.5$  meters.

of the development.

“PS3 HMI.vi” was the first one created, directly derived from Skåtun’s work. It contains and require the bare minimum to manually control CSE1 through a PS controller. To run it requires, LabVIEW with SIT package, BTSix and PPJoy installed and the .vi file, the .mdl file or it’s derived files, a wireless network, a PS controller with Bluetooth and Dongle. In theory this enables CSE1 to not be confined to only the MC Lab.

“Thruster HMI.vi” was deveploed for the purpose of measuring the thruster forces produced. The input values needed to be fixed over a period. It is an expansion of “PS3 HMI.vi”, allowing direct thruster control from the Front Panel.

“StudentHMI.vi” is one of the last version of the GUI and the one who is most similar to Skåtun’s program of the four. It can also be viewed as a simplified version of “Template HMI.vi”. It was created for the avarage student to easily use and modify. It contains a manual PS thruster control, a Dynamic Positioning (DP) control with setpoint, and a Control Lyapunov Function (LgV) control with linear and ellipse path.

“Template HMI.vi” is the final product and will be the main focus. It is a mostly generic GUI, with a setup for manual PS thruster control, two automated control systems with the option of linear or ellipse path or setpoint. It is in essence the same as Skåtun’s program, see Skåtun (2011) for a simple introduction. It requires data from qualisys to make use of the automated control systems.

## 2.5.2 Front Panel

This is where the operator interacts with the rest of the programs when using **CSE1**. The panel is directly connected to the **Block Diagram**, and vertically divided into two parts.

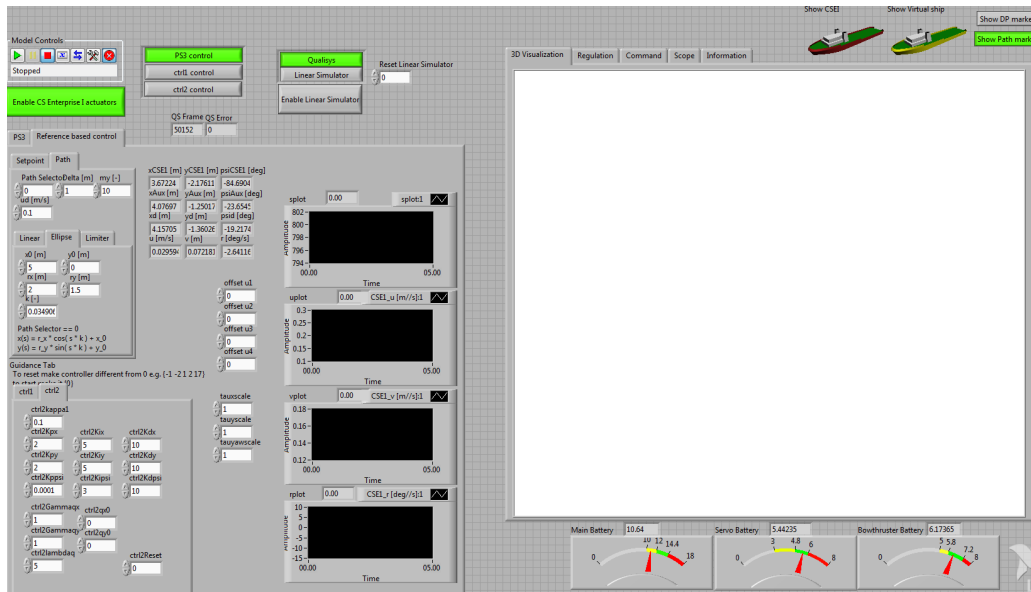


Figure 2.3: Overview of **LabVIEW** Front Panel.

The left part contains the dials, switches, indicators and controls for input and selections. To switch between the different control mode, use the “radio button column” located on top in the middle. It is mapped to a constant block in the **.mdl** file, sending an integer from 0 and up. That value is then used in a switch-block to determine which input to use. Similarly for which input to pass to the controller, the “radio button column” above the “Enable Linear Simulator” boolean button.

The tabs are used for compact structuring. The right half are different types of visualization of the process taking place in the background, a 3D visualization, and plots of key variables. The various controls, indicators and plots should be self-explanatory based on the name label.

## 2.5.3 Block Diagram

This is where the each element in the **Front Panel** is defined with respect to interaction, behavior and data to display among one another. In general it is here the mapping are done. However, since the model structure and dynamics are created in **Simulink** the true mapping happens in **SIT**, which in turn automatically create the mapping in the **Block Diagram**

The diagram is basically the same as Skåtun’s. It have been organized and tweaked for relative path definition, and with added comments and lables. It can be divided into four

main groups. First is the loop structure that handles the signals from the **PS** controller via **BTSix** and **PPJoy**. Second is the blocks used for the 3D visualization. The third group is the structures created by **SIT**. The last group is the miscellaneous group scattered all across the diagram containing tab-, control-, and unmapped-blocks. Unless they are wired to anything they can be more or less freely be placed anywhere in the diagram.

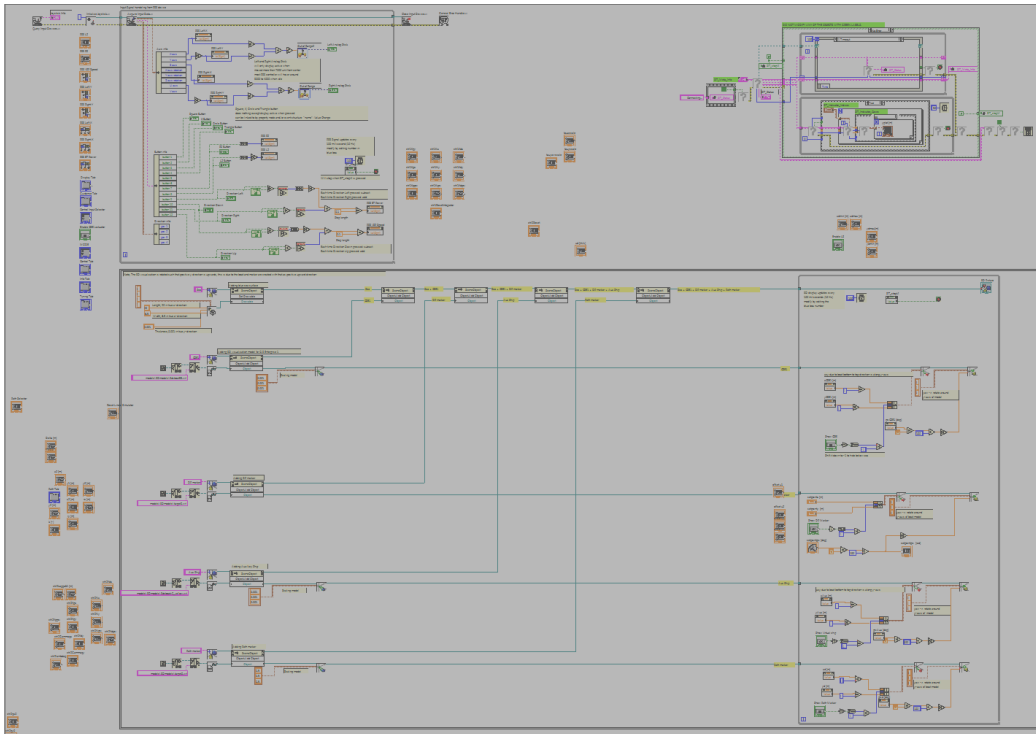


Figure 2.4: Overview of **LabVIEW** Block Diagram.

#### 2.5.4 Simulation interface toolkit

**SIT** is the intersection that connects **LabVIEW**(**Block Diagram** and **Base\_Rate\_Loop.vi**) , **Simulink**, **CSE1** and **Qualisys** together. It connects to **.mdl** file or the derived files (**.dll/vxworks**) in “Model and Host”. In “Mappings” the connection between the blocks in **Block Diagram** and the blocks in **.mdl** file is established. The relationship of the **SIT** output block in **.mdl** with (**CSE1**) the thrusters through **cRIO** are set in “Hardware’ I/O” in connection with the **FPGA** bitfile. As well as the **SIT** input block in **.mdl** for the battery voltages and any force ring connected to the **cRIO**. The link between **Qualisys** and the remaining **SIT** input block in **.mdl** is done indirectly through **IO.llb** and **Base\_Rate\_Loop.vi**.

The **IO.llb** is automatically created by **SIT**. It contains six **.vi** files, **Base\_Rate\_Loop.vi**, **Close-**, **Init-**, **Read-**, **Write.vi** and **Ref.ctf**. It is in **Base\_Rate\_Loop.vi** the whole **Qualisys** data acquisition is handled. The others are called, but it is not worth going into detail. **Base\_Rate\_Loop.vi** makes use of a **driver.vi** created by Senior Engineer Torgeir Wahl.

### 2.5.5 Qualisys Track Manager Drivers

The original driver used in [Skåtun \(2011\)](#), also created by Torgeir Wahl, acquired, processed and sent the data all in the same timestep. The consequence of this forced the time step of the `.mdl` to be the same as the sample rate of `Qualisys`.

If `Qualisys` had a higher sample rate than the rate the `.mdl` file was solved, the `.mdl` file would constantly be working with older and older data as the time progressed. If the `.mdl` file had a higher frequency than `Qualisys`, the `Base_Rate_Loop.vi` would crash ending the run. This is caused by the driver not having any data to pass on and nothing is sent to the `.mdl`.

The original driver also contained an error where the size of the output array was smaller than the actual size. This caused the shuffling of the data set. Even if both `Qualisys` and `.mdl` were both set to the same frequency, it would have only been a matter of time before `.mdl` in a time step began ahead of `Qualisys`. This is due to that each of them have their own internal clock, that is not synchronized. When the difference between the two becomes too large, `Base_Rate_Loop.vi` crashes.

Most runs could not last longer than a few minutes and this was the main problem. As each crash meant a total reboot of `LabVIEW`, combined with the lost of connection, most of the time was spent on establishing and deploying the software.

To fix this problem, a Producer/Consumer design pattern was implemented. The Producer (`QTMTask.vi`) and Consumer (`QTMdriver_....vi`) replaced the original `QTMdriver.vi`. `QTMTask.vi` follows `Qualisys` frequency, and `QTMdriver_....vi` follows real-time target frequency (`.mdl` file).

This setup makes them frequency independent of each other. `QTMdriver.vi` acquires the data using other `.vi` files and add it to a shared memory block (data queue) it have with `QTMdriver_....vi`. `QTMdriver_....vi` retrieves the data set from the data queue, wipes the queue clean, passes the data set on to the `SIT` server and stores the data in a memory block. If there is no new data set, most of the data set in the memory block is passed to the `SIT` server instead, analog to a zero order hold. This setup greatly improves the reliability and robustness of the system.

For more information, [National Instruments \(n.d.b\)](#) and [National Instruments \(n.d.a\)](#).

## 2.6 Simulink

The control architecture is defined in the `Simulink` diagram. As previously mentioned the mapping between `Simulink` and `LabVIEW` is handled by `SIT`. The blocks utilized for the actual routing are “Constant”-blocks for signals from `LabVIEW` (Controls), and “Gain”-blocks for signals to `LabVIEW` (Indicators).

The names given to the “Controls” in `LabVIEW` are set to be similar if not exactly the same as their counterpart in `Simulink` (“Constant”-blocks). An example, The “Control” that determines which controller to use is called “Mode Control” in `LabVIEW`. It’s counterpart, meaning the “Constant”-block it shall be mapped to in the `Simulink` diagram, is given the name “Mode Control Selector”. This simplifies the process when the mapping is done



in **SIT** Connection Manager, making it easier to know which “Control” or “Indicator” to mapped to which block.

The values set on the “Constant”-blocks are often set to the default value preferred. However those values does not matter when running the it via **LabVIEW**, since the **.vi** will send the signal which the **Simulink** diagram will update with before executing. The values set in the “Gain”-blocks will be multiplied with the signal before sending it to **LabVIEW**, if mapped. Therefore most often those values are set to one.

The latest versions utilize “GoTo”- and “From”-blocks, with global variables, to pass values between subsystems. The previous versions used wires to send signals between the subsystems. This created a lot of clutter and unnecessary work when adding, removing or just moving blocks due to the path the wires would be automatically placed.

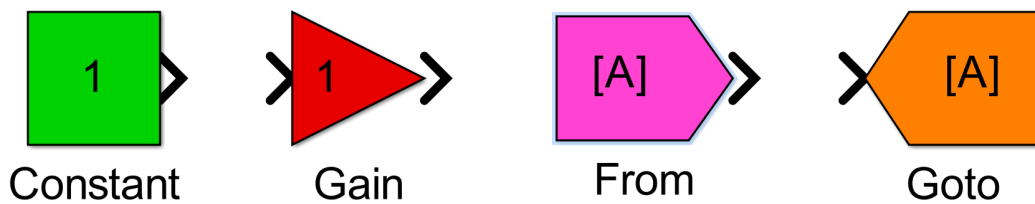


Figure 2.5: Blocks used for signal routing and mapping in **Simulink** diagram.

This enables most blocks to be placed anywhere in the **Simulink** diagram. However, for structure and logical flow when looking at the it, the blocks are placed as if they were using wires and parts placed in subsystems where it is logical. In general the diagram can be read from top to bottom, and from left to right.

The top level contains four blocks, where three of them are subsystems. The “SignalProbe”-block is the port for communication with the **SIT** server. All values mapped from **LabVIEW** are gathered in the subsystem “Input from LabVIEW”. Every signal mapped to **LabVIEW** are located in the “Output to LabVIEW” subsystem. Each inputs from **SIT** are in the subsystem “ Input from SIT” found under “Main Subsystems/Navigation”. Outputs to **SIT** are within the subsystems located in “Main Subsystems/Plant/CSE1 actuator”. The block are color coded, where green means “Source”, red means “Sink”, orange means “GoTo”, and magenta means “From”.

The solver used is ode5 (Dormand-Prince), with 0.1 as fixed-step size. Other solvers can also be used, it depends on the complexity of the system, and if the solver is able to finish within the time step. When compiling the file using **Real-Time Workshop**, the only way to set the frequency of the model is by choosing fixed-step. If variable-step is chosen then **Real-Time Workshop** will decide the frequency.

A small sidenote: Some comments and names of blocks in the **.mdl**-files may not be up to date for what itthey are actually used for.

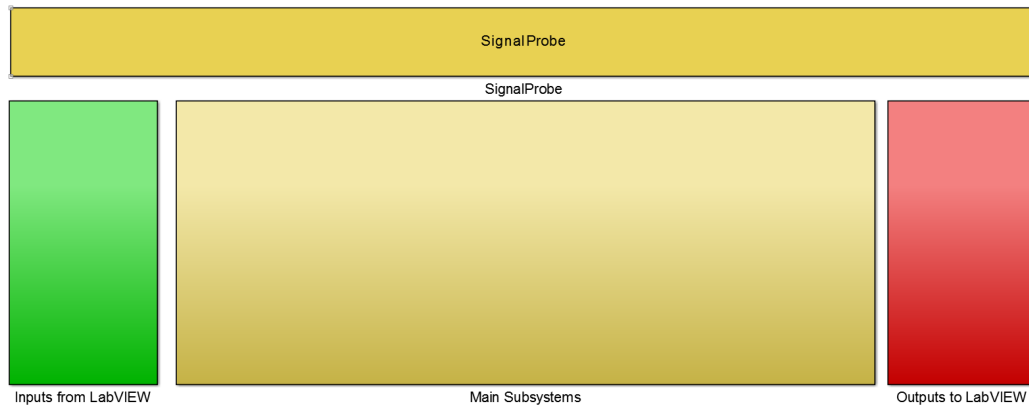


Figure 2.6: Top level in **Simulink** diagram.

### 2.6.1 Input from LabVIEW

The function of this subsystem is to gather all input mappings from **LabVIEW** in one place. It consists of “Constant”-blocks to map to, and “GoTo”-blocks to declare them as global variables. The signals mapped here are structured into scalar, vector or matrix depending on the application of the signal before being declared a global variable.

### 2.6.2 Output to LabVIEW

This subsystems functions is similar to the “Input from LabVIEW”, it gathers all mapping in one place, just for outputs instead. It consists of “From”-blocks obtaining the signals from the global variables, and divides most of them into scalars for mapping. The “Gain”-blocks are the counterpart of the “Indicators” in **LabVIEW**.

### 2.6.3 Guidance

The “Guidance” module’s main function is to generate all the reference or desired variables the controllers needs. It contains e a “Path”-, “Heading”-, “Speed assignment”- and “Line-Of-Sight”-module.

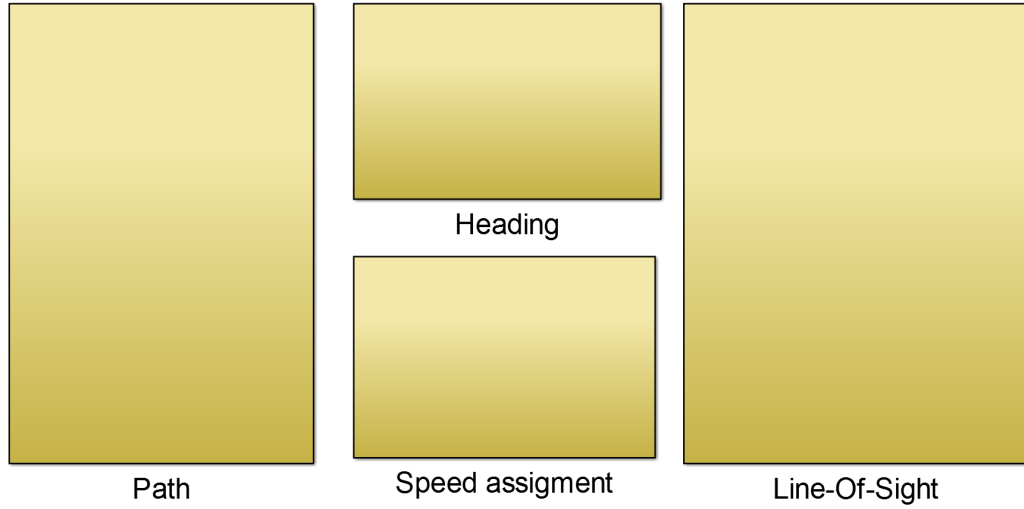


Figure 2.7: “Guidance” module in the [Simulink](#) diagram.

Guidance module input		
pathSelector	[-]	Switch workaround parameter for path
$s$	[-]	Path parameter of desired path $p_d$
$x_0$	[m]	x-coordinate of origin of ellipse path in $Q$ -frame
$y_0$	[m]	y-coordinate of origin of ellipse path in $Q$ -frame
$r_x$	[m]	Radius of ellipse path in x-direction in $Q$ -frame
$r_y$	[m]	Radius of ellipse path in y-direction in $Q$ -frame
$k$	[-]	Scaling parameter of path parameter $s$
$x_1$	[m]	x-coordinate of linear path in $Q$ -frame when $s$ is zero
$y_1$	[m]	y-coordinate of linear path in $Q$ -frame when $s$ is zero
$x_2$	[m]	x-coordinate defining heading of linear path in $Q$ -frame
$y_2$	[m]	y-coordinate defining heading of linear path in $Q$ -frame
$u_d$	[m/s]	Desired surge speed in $B$ -frame
$q$	[m]	Virtual point-mass coordinates of vessel in $Q$ -frame
$\Delta$	[m]	Lookahead distance
$\mu$	[-]	Tuning parameter for $s$ gradient algorithm

Guidance module output		
$\chi$	col([m],[m],[rad])	3DOF reference vector in $\mathcal{Q}$ -frame, col( $\mathbf{q}, \psi_{los}$ )
$\chi^q$		Partial differentiation of $\chi$
$\chi^s$		Partial differentiation of $\chi$
$\psi_{los}^q$	[rad/m]	Partial differentiation of $\psi_{los}$
$\psi_{los}^{q^2}$	[rad/m <sup>2</sup> ]	Partial differentiation of $\psi_{los}$
$\psi_{los}^{qs}$	[rad/m]	Partial differentiation of $\psi_{los}$
$\psi_{los}^s$	[rad]	Partial differentiation of $\psi_{los}$
$\psi_{los}^{s^2}$	[rad]	Partial differentiation of $\psi_{los}$
$f_q$		Dynamic LOS assignment for $\dot{q}$
$f_q^q$		Partial differentiation of $f_q$
$f_q^s$		Partial differentiation of $f_q$
$f_q^t$		Partial differentiation of $f_q$
$f_s$		Dynamic LOS assignment for $\dot{s}$
$f_s^q$		Partial differentiation of $f_s$
$f_s^s$		Partial differentiation of $f_s$
$f_s^t$		Partial differentiation of $f_s$

## Path

The “Path” module’s main function is to generate desired position  $\mathbf{p}_d$ . Continuous parameterization of the paths are implemented in this module. It have three modules, one for linear path, one for ellipse path and a workaround switch. Both paths are created simultaneously using the same path parameter  $s$ . However  $s$  will only be dependent on the chosen path.

The linear path is created with:

$$x = (x_2 - x_1)s + x_1 \quad (2.1a)$$

$$x^s = (x_2 - x_1) \quad (2.1b)$$

$$y = (y_2 - y_1)s + y_1 \quad (2.1c)$$

$$y^s = (y_2 - y_1) \quad (2.1d)$$

$$(2.1e)$$

where  $x_1$  and  $y_1$  are coordinates of linear path in  $\mathcal{Q}$ -frame when  $s$  is zero, and  $x_2$  and  $y_2$  defines the heading of linear path in  $\mathcal{Q}$ -frame. The higher order partial differentiations are set to 0.

The ellipse path is created with:

$$x = r_x \cos(ks) + x_0 \quad (2.2a)$$

$$x^s = -r_x k \sin(ks) \quad (2.2b)$$

$$x^{s^2} = -r_x k^2 \cos(ks) \quad (2.2c)$$

$$x^{s^3} = r_x k^3 \sin(ks) \quad (2.2d)$$

$$y = r_y \sin(ks) + y_0 \quad (2.2e)$$

$$y^s = r_y k \cos(ks) \quad (2.2f)$$

$$y^{s^2} = -r_y k^2 \sin(ks) \quad (2.2g)$$

$$y^{s^3} = -r_y k^3 \cos(ks) \quad (2.2h)$$

$$(2.2i)$$

where  $x_0$  and  $y_0$  are coordinates of origin of ellipse path in  $\mathcal{Q}$ -frame,  $r_x$  and  $r_y$  are radius of ellipse path and  $k$  is a scaling parameter of path parameter  $s$ , often much smaller than 1.

The values are merged together into  $\mathbf{p} = \text{col}(x, y)$  for each of their respective partial differentiations, and the module implements equation (36) in Skjetne (2014).

The workaround module is used due to unknown technical limitations that wont running or compiling when a regular “Switch”-block for switching between paths. It uses a variable dubbed “pathSelector” that can be either 1 or 0. The workaround make use of

$$\mathbf{p}_d = \mathbf{p}_{d1} \text{pathSelector} + \mathbf{p}_{d0} (1 - \text{pathSelector}) \quad (2.3)$$

For each partial differentiations, where  $\mathbf{p}_d$  is the chosen path,  $\mathbf{p}_{d1}$  is the linear path and  $\mathbf{p}_{d0}$  is the ellipse path. If “pathSelector” is 0, then ellipse path is chosen. If it is 1, then linear path is chosen.

## Heading

The “Heading” module make use of the outputs from the “Path” module. It implements equation (2) and (47) to (49) in Skjetne (2014), and outputs the desired heading  $\psi_d$  and it’s partial differentiations,  $\psi_d^s$  and  $\psi_d^{s^2}$ .

## Speed Assigment

The “Speed Assigment” module require the outputs from the “Path” module, in addition to the desired forward speed  $u_d$ . It implements eappropriatequation (5), (38) and (39) in Skjetne (2014), and passes on the speed assigment  $v_s$ , it’s partial differentiations and the time derivative of  $u_d$ .

## Line-Of-Sight

The “Line-Of-Sight” module’s main function is to generate the 3DOF reference vector  $\chi$ . It takes in the outputs from the previous modules, in addition to the lookahead distance  $\Delta$ , tuning parameter for  $s$  gradient algorithm  $\mu$  and the virtual point-mass coordinates in  $Q$ -frame  $q$ . Equation (6) to (8), (40) to (46) and (50) to (70) in Skjetne (2014) are implemented here. Its outputs are  $\chi$ , dynamic LOS assignment for  $\dot{q}$ ,  $f_q$ , and dynamic LOS assignment for  $\dot{s}$ ,  $f_s$ .

### 2.6.4 Control

The “Control” module’s main function is to generate a 3DOF command output  $\tau$  and a set of thruster commands  $T_c$ . It is currently made up of five modules, one switch, one thruster allocation, and three control module. It is set up to handle three controllers, but can be expanded by adding and increasing the number of ports in the switch.

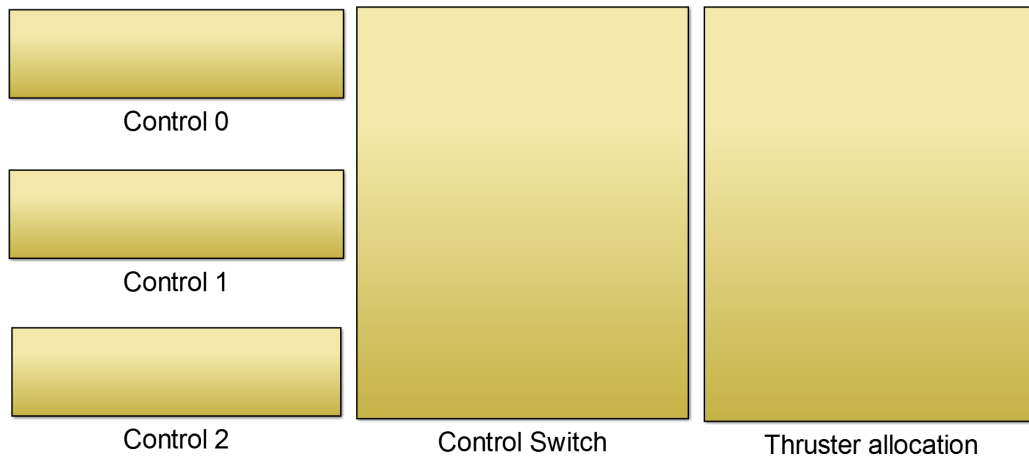


Figure 2.8: “Control” module in the Simulink diagram.

Control module input		
controlModeSelector	[-]	Parameter for switching between controllers
ctrlReset	[-]	Parameter for resetting controllers
$s_0$	[-]	Initial value of $s$
$q_0$	[m]	Initial values of $q$
$\eta_d$		Desired position and orientation in $Q$ -frame
$\eta$		Position and orientation in $Q$ -frame
$\nu$		Velocities in $B$ -frame
$\chi$		3DOF reference vector in $Q$ -frame, $\text{col}(q, \psi_{los})$
$\chi^q$		Partial differentiation of $\chi$
$\chi^s$		Partial differentiation of $\chi$
$\psi_{los}^q$		Partial differentiation of $\psi_{los}$
$\psi_{los}^{q^2}$		Partial differentiation of $\psi_{los}$
$\psi_{los}^{qs}$		Partial differentiation of $\psi_{los}$
$\psi_{los}^s$		Partial differentiation of $\psi_{los}$
$\psi_{los}^{s^2}$		Partial differentiation of $\psi_{los}$
$\psi_{los}^s$		Partial differentiation of $\psi_{los}$
$f_q$		Dynamic LOS assignment for $\dot{q}$
$f_q^q$		Partial differentiation of $f_q$
$f_q^s$		Partial differentiation of $f_q$
$f_q^t$		Partial differentiation of $f_q$
$f_s$		Dynamic LOS assignment for $\dot{s}$
$f_s^q$		Partial differentiation of $f_s$
$f_s^s$		Partial differentiation of $f_s$
$f_s^t$		Partial differentiation of $f_s$
$M$		Inertia matrix
$D$		Hydrodynamic damping matrix
$B$		Thruster configuration matrix
$K_P$	[-]	Diagonal tuning matrix
$K_I$	[-]	Diagonal tuning matrix
$K_D$	[-]	Diagonal tuning matrix
$\Gamma_q$	[-]	Diagonal tuning matrix
$\kappa_1$	[-]	Tuning parameter for virtual control $\alpha$
$\lambda$	[-]	Gradient update law tuning parameter
$AS_{LY}$	[-]	Up/Down position of Left Analogstick
$AS_{LX}$	[-]	Left/Right position of Left Analogstick
$AS_{RY}$	[-]	Up/Down position of Right Analogstick
$AS_{RX}$	[-]	Left/Right position of Right Analogstick
L2	[-]	Shoulder botton signal
R2	[-]	Shoulder botton signal
Bow Thruster (BT) power	[-]	BT power limit
VSP speed	[-]	VSP speed setpoint

Control module output		
$\boldsymbol{\tau}$		Force vector in $\mathcal{B}$ -frame
$\mathbf{T}_c$		Thruster commands set
$s$	[-]	Path parameter of desired path $p_d$
$\mathbf{q}$	[m]	Virtual point-mass coordinates of vessel in $\mathcal{Q}$ -frame

### Control #n

Within each “Control #n” different kind of control design can be implemented, for modularity and structure one per subsystem. However, they can be placed anywhere as long as it uses a “GoTo”-block to declare the  $\boldsymbol{\tau}$  produced as a global variable with a unique variable name, and use a “From”-block in the “Control Switch” module to retrieve. For automated controls; reference values, tuning parameters,  $\boldsymbol{\eta}$  and  $\boldsymbol{\nu}$ .

“Control 0” is used for the direct thruster control through a PS controller. It need the x- and y-coordinate of each analog stick, R2 and L2 signal, and BT power limit and VSP speed setpoint to create  $\mathbf{T}_c$ .

For a DP PID controller; The desired position and orientation  $\eta_d$ , vessel dynamic matrices  $\mathbf{M}$  and  $\mathbf{D}$ , tuning matrices  $\mathbf{K}_P$ ,  $\mathbf{K}_I$  and  $\mathbf{K}_D$ , and  $\boldsymbol{\eta}$  and  $\boldsymbol{\nu}$  are needed as inputs.

For the LgV2 and NLPID design from Skjetne (2014); all the outputs from “Guidance” , a control reset variable called “ctrlReset”, initial values  $s_0$  and  $q_0$ , vessel dynamic matrices  $\mathbf{M}$  and  $\mathbf{D}$ , tuning parameters and matrices  $\kappa_1$ ,  $\boldsymbol{\Gamma}_q$ ,  $\lambda$ ,  $\mathbf{K}_P$ ,  $\mathbf{K}_I$  and  $\mathbf{K}_D$ , and  $\boldsymbol{\eta}$  and  $\boldsymbol{\nu}$  are needed as inputs. Their outputs are  $\boldsymbol{\tau}$ , virtual point  $\mathbf{q}$  and path parameter  $s$ .

### Control Switch

The “Control Switch” module is a straight forward subsystem with a “Switch”-block. It takes in the  $\boldsymbol{\tau}$ ’s from the controller modules, and a variable named “controlModeSelector” to decide which controller to use. The “Switch”-block is zero-based, since the “ControlMode” “radio button” in LabVIEW is zero-based.

### Thruster allocation

The “Thruster allocation” module converts  $\boldsymbol{\tau}$  into  $\mathbf{T}_c$ , in two steps. First

$$\mathbf{f}_{act} = \mathbf{B}^+ \boldsymbol{\tau} \quad (2.4)$$

where  $\mathbf{f}_{act} = \text{col}(f_1, f_2, f_3, f_4, f_5)$  is the force actuator vector,  $\boldsymbol{\tau}$  is the force vector in  $\mathcal{B}$ -frame, and  $\mathbf{B}^+$  is the pseudoinverse of the thruster configuration matrix  $\mathbf{B}$ .

Then  $\mathbf{f}_{act}$  is mapped to thruster inputs  $\mathbf{u}$  through lookup tables, before merging with the BT power limit and VSP speed setpoint to create the thruster commands set  $\mathbf{T}_c$ . If other power limit or speed setpoint is desired by the user, then the lookup tables needs to be replaced with the appropriate ones. This part is hardcoded into the control architecture. For details on the lookup tables see system identification section.



### 2.6.5 Plant

The “Plant” module’s main function is to make use of  $\tau$  and  $T_c$ , and directly or indirectly produce  $\eta$  and  $\nu$ . It is divided into two subsystems, “Real Target” and “Simulator”.



Figure 2.9: “Plant” module in the [Simulink](#) diagram.

Plant module input		
controlModeSelector	[-]	Parameter for switching between controllers
enableCSE1	[-]	Parameter to enable the thruster subsystems
LS_Enable	[-]	Parameter to enable the Linear simulator
$\tau$		Force vector in <b>B-frame</b>
$T_c$		Thruster commands set
TC#n		Direct thuster command set from control
$M$		Inertia matrix
$D$		Hydrodynamic damping matrix
LS_Reset'	[-]	Parameter for resetting linear simulator
$\eta_0$	[-]	Initial values of $\eta_{LS}$
$\nu_0$	[m]	Initial values of $\nu_{LS}$
Plant module output		
$\eta_{LS}$		Position and heading form linear simulator
$\nu_{LS}$		Velocities from linear simulator

#### Real Target

The “Real Target” uses the  $T_c$  output from the “Control”-module, and convert them into signals that each thruster is able to follow. It needs three input signals  $T_c$ , “controlModeSelector” and an enabling variable “enableCSE1” to enable the thruster subsystems. The creation and tuning of those subsystems are documented in [Skåtun \(2011\)](#). According to

Skåtun, the 2D lookup tables should counteract the circular motion of each servo, and create a linear movement of the **VSP** control sticks. The only thing different from the original is the modularize structure.

There is a workaround for the  $T_c$ , to account for controllers that are direct thruster controls TC#n, if they are implemented in the “Control” module. However manual adjustment and check is needed to make sure the workaround corresponds to the right controller.

This subsystem does not directly produce  $\eta$  and  $\nu$ , since it just sends command signals to a **cRIO**, who in turn routes the signal where they need to go. The  $\eta$  and  $\nu$  are calculated in the “Naviagtion” module.

### Simulator

The “Simulator” does not make use of the thrusters, instead it runs on a linear vessel dynamics model presented in the introduction, equation (1.1). It needs,  $\tau$ ,  $M$ ,  $D$ , an enable parameter, “LS\_Enable, a reset parameter “LS\_Reset”, intial position and heading  $\eta_0$ , intial velocities  $\nu_0$ . The outputs are  $\eta_{LS}$  and  $\nu_{LS}$

### 2.6.6 Navigation

The “Navigation” module’s main function is to calculate and output  $\eta$  and  $\nu$ . It consists of “Input from SIT” and “Navigation Switch”.

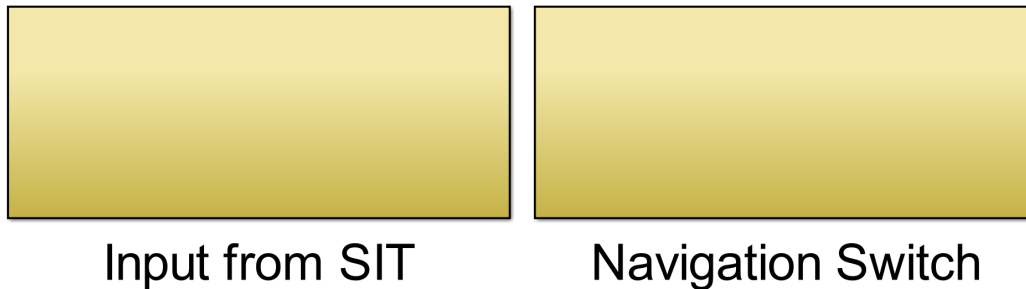


Figure 2.10: “Navigation” module in the **Simulink** diagram.

#### Input from SIT

This subsystem have remained mostly the same since the orginal subsystem found in **Skåtun (2011)** . The major difference is the passive low speed observer used to estimate the velocities instead. Its function is to process the **Qualisys** values received through the **SIT** server, and output  $\eta_{QS}$  and  $\nu_{QS}$ . In addition it needs  $T_c$ ,  $M$ ,  $D$  for the observer. It also sends out other parameters given by **Qualisys**, seperatly battery voltages

The passive low speed observer was introduced into the stucture by Co-advisor Øivind Kjerstad, due to the noisy velocities created when using a “Derivation”-block. It is a modified version of an observer from **MSS GNC** Toolbox.

### Navigation Switch

The “Navigation Switch” is similar to “Control Switch”. it uses a variable called “controlInputSelector” to decide if it shall send the value from **Qualisys** or the simulator. The additional inputs are  $\eta_{LS}$ ,  $\eta_{QS}$ ,  $\nu_{LS}$  and  $\nu_{QS}$ . The outputs are  $\eta$  and  $\nu$ .

### 2.6.7 C/S Enterprise 1 Matrices

The function of this subsystem is to define **CSE1**’s matrices. it is created to make it easy and efficient to modify , without having to check if all the places the matrices are used are up to date. It does not have any inputs, but it is possible to directly map controls from **LabVIEW** here to provide an realtime way to change the matrices’ values. Its output are, **M**, **D** and **B**.

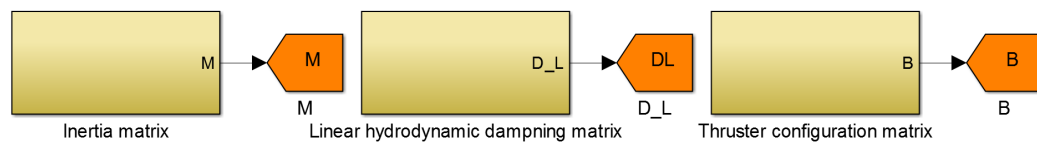


Figure 2.11: “C/S Enterprise 1 Matrices” module in the **Simulink** diagram.

### 2.6.8 Data logging

The point of data log was chosen in **Simulink** since it is the performances of the control system that are of interest. Each barrier between the point of interest and point of measuring is a potential source of error and delay. However, this approach requires the operator to manually extract the log file if the **.mdl** file was running on the **cRIO** through the “Measurement & Automation Explorer”. The data is stored in **.mat** formate using a “ToFile”-block, which is generated and stored in the workspace wherever the model is running (Execution Host). The name of the data file is set in the dialog window of the “ToFile”-block.

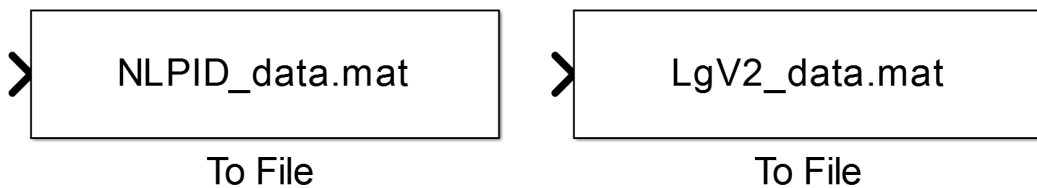


Figure 2.12: Two “ToFile”-blocks used in **Simulink** diagram.



## Chapter 3

# System identification

For the system identification arrangement twelve rotation free hook, three force ring and three springs were used. Two force rings on portside and two springs on starboard side, and one force ring in the aft and a spring at the bow.

In general each measurement series last 30 seconds, with 30 seconds in between measurement to allow the surface disturbance to die out and reset the zero settings. The first measurement set did not have a zero measurement before the disturbance is introduced, e.g. towing or activating **CSE1**, which was introduced in the latest measurement set.

The first set of measurements was done for towing the hull 0, 45 and 90 degrees, **VSP** force generation with a VSP speed set to 0.4 with 0.1 step size, and for **BT** with power limit at 0.5 also 0.1. For the thrusters the input value ranged from -1 to 1.

The second set were done just for the thrusters for lower speed and power. VSP speed for 0.2 and 0.3 and BT power at 0.15, 0.3, 0.4 and 0.5.

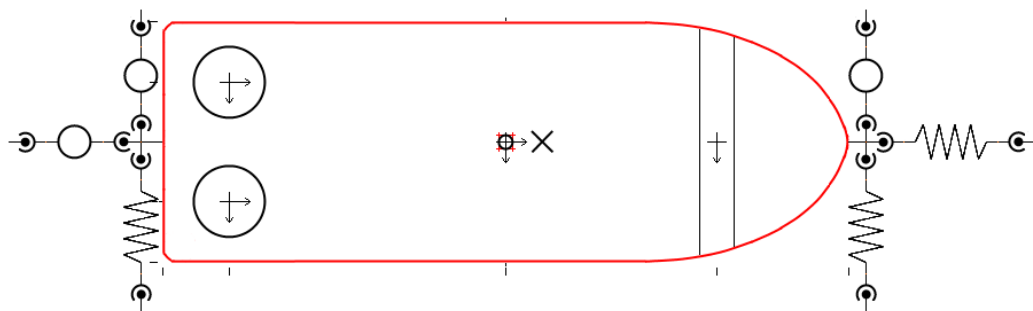


Figure 3.1: The setup of **CSE1** for system identification.

### 3.1 Hull

The measurements from 0 and 90 degrees towing yielded:

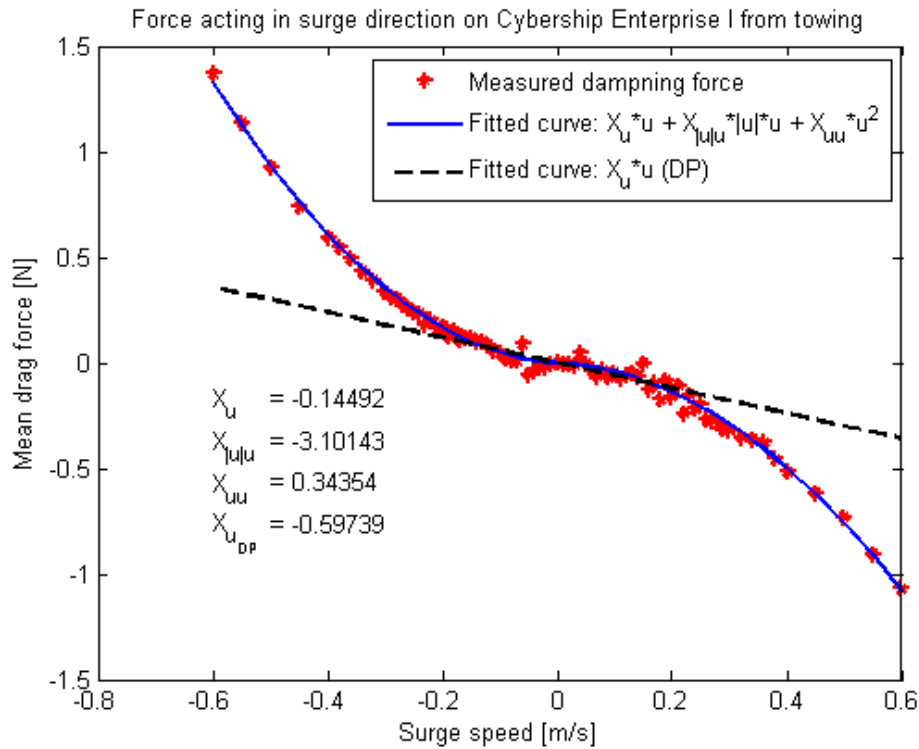


Figure 3.2: Measurements of damping coefficient of CSE1

The values for  $X_u$  and  $Y_v$  are similar to Skåtun's values. And a new value can be added for slow speed  $N_v = 0.18140$ .

### 3.2 Thruster mapping

The VSP have been measured for 0.2, 0.3 and 0.4 in VSP speed, while the BT have been measured for 0.15, 0.3, 0.4 and 0.5 in power limit.

The starboard voith schneider propeller rotates slow than the port voith schneider propeller. The effect is notiable in the meaurment. However it does not come into effect unless

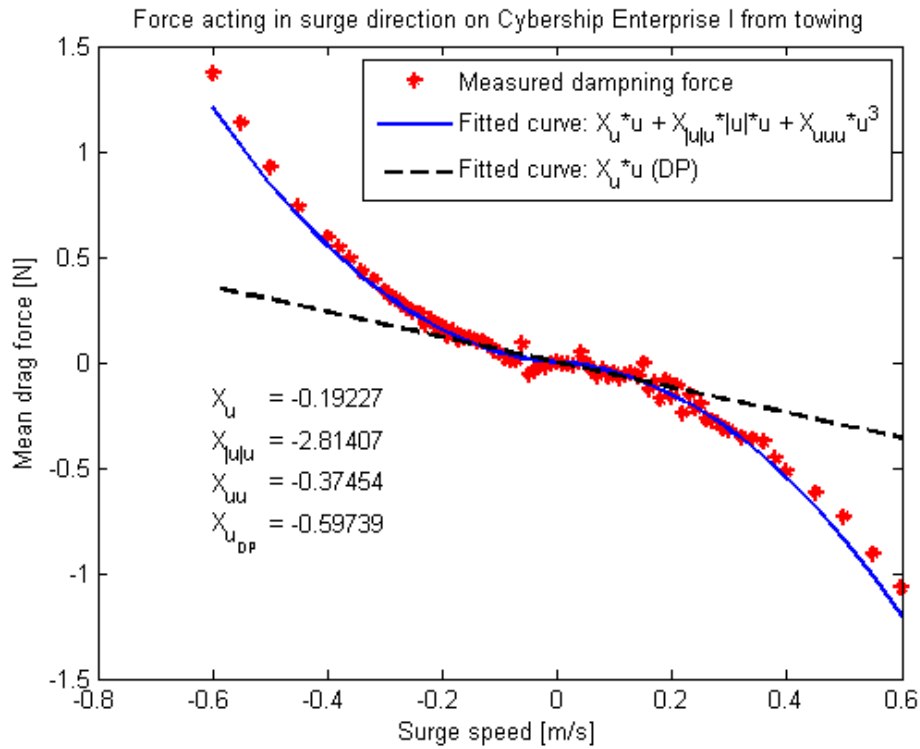


Figure 3.3: Measurements of damping coefficient of CSE1

the maximum force are required, and it becomes less significant as higher rotation speed are used. It is also noted that the servos are significantly coupled and the force output drops at the periphery value, 1. It can be seen from the thruster measurements that the lookup tables for the voith schneider propellers does not truly cancel out the circular motion of the servos. Some of it can be caused by the rotation when measuring, or due to placement of thruster. However this can not fully explain the notable force measured in the other direction. Of the servos, servo 4 have the strongest coupling in surge-sway.

During the measurement of the thrusters it is noted that the thruster commands have an error of margin around 0.03. Meaning the 0.21, 0.22 and 0.23, can generate the same force. See appendix for plots.

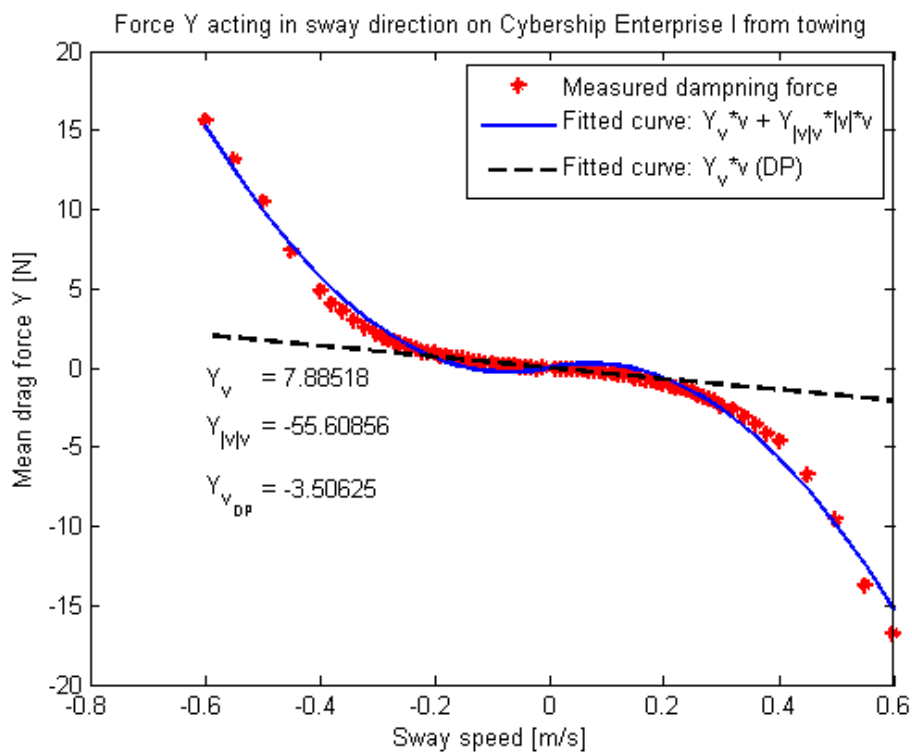


Figure 3.4: Measurements of damping coefficient of CSE1



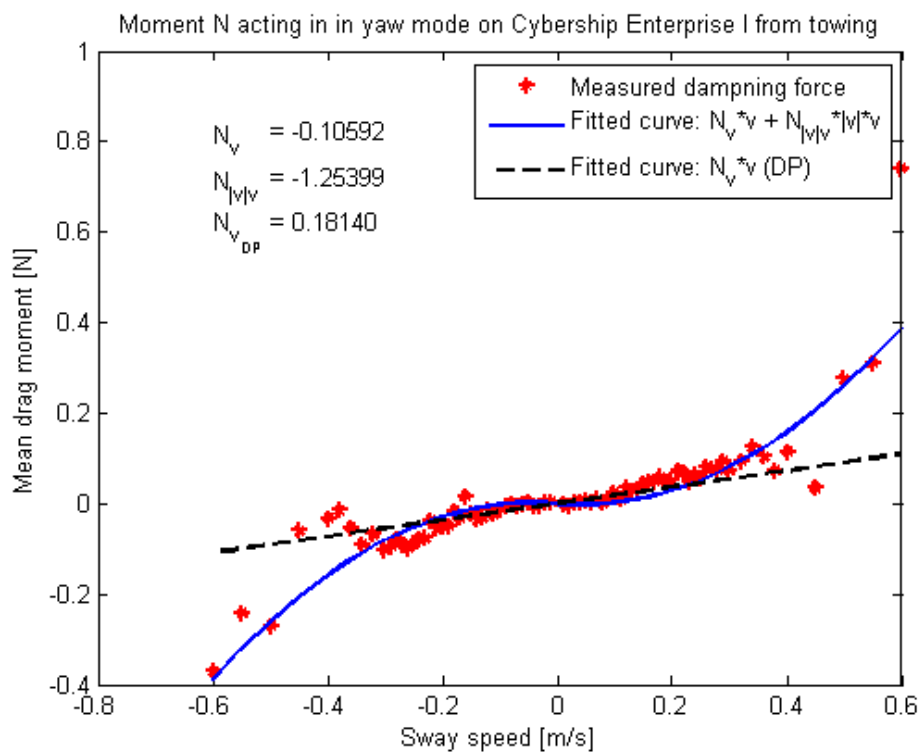


Figure 3.5: Measurements of damping coefficient of CSE1



## Chapter 4

# Line of Sight Experiments

As previously mentioned the two controllers implemented are from [Skjetne \(2014\)](#).

Two advance control design were implemented, tuned and tested, a *LgV backstepping* and a *Nonlinear PID* designed controller. Only ellipse path was used in the laboratory. This had to do with space constraints, and a wish to have long run time on the experiments.

The gradient optimization finds the fastest or steepest change, this helps the controller converge faster toward the desired setpoint. An unfiltered update law can be sensitive to noise in the measurement, while a filtered update law would smoothen out and therefore be more stable with noisy measurements. However this will introduce a delay.

The controllers are designed with three points that chases each other, the path point  $\eta_d$ , the virtual point  $\chi$  and the vessels point  $\eta$ .  $\eta_d$  stays on the path and moves to minimize the distance between it and  $\chi$ .  $\chi$  tries first to minimize the distance between it and  $\eta_d$  before  $\eta$ . While  $\eta$  will only converge to  $\chi$ . If the filtered update law is disabled controller becomes a tracking case.

Attached electronically are the data from the runs, but due to timeconstraint those are not presented here.

### 4.1 Simulation runs

In the ideal simulated world both of them were equal in terms of maneuvering, both for linear paths and for ellipse path. Depending on the tuning their initial transient behavior can be erratic and unnatural.

### 4.2 Laboratory runs

Originally only the *LgV backstepping* was tested in the laboratory. It converged and performed well. The only downside was it would constantly overshoot the heading, resulting in a constant oscillation, while moving along the path. The reason was due to the noisy velocity estimation.

Other opportunity presented itself to run more experiments in the laboratory, However, unknown at that time and discovered to late, one of the servo arms broke due to fatigue from the constant oscillation of the previous runs, corruping the mapping and observer estimates. In the laboratory, their performance depended heavily on how they were implemented. If both of them were fully implemented, *LqV backstepping* proved to handle the uncertainties better. Although it would overshoot when exiting the sharper part of the ellipse path. The vessel is able to follow the virtul point it is chasing, but the virtual point is unable to stick to the desired path. While the fully implemented *Nonlinear PID* would struggle to converge to the path and behave erratic. The velocity dependent term distorted *Nonlinear PID*'s results the most . The reason is most likely due to the quality of the estimations of the velocities from the observer. The feedforward term also deteriorate the control, and prevents it from converging.

If the *Nonlinear PID* was partially implemented, deactivating the feedforward and the velocity dependent term, then it is the superior one. It would converge naturally to the desired position. Once on, it would stay there indefinitely despite of the broken servo arm.

## Chapter 5

# Conclusion

The reliability when conducting laboratory experiments with CyberShip Enterprise 1 have greatly improved. This was achieved through repositioning and replacing the antenna for wireless communication, and a restructuring of how signals were handled between servers and softwares. The original setup with single frequency was replaced with a multi-frequency producer-consumer structure.

The futherst away a vessel is visible for Qualinsys is around 17 meters from the cameras. The shortest distance is roughly 4 meters infront of the cameras. This result in a lengthwise workspace for a vessel to be in the range of 13 meters. This length length can be increased to 27 meters, If the carriage start from the beach end, and moves toward the wavemaker during the experiment. It is not possible to increase it futher due to the length of the basin, the wavemaker, beach, in/outlet and carriage is occupying.

In the system identification, an addtional hydrodynamic damping coefficient for slow speed have been determined for the hull ( $N_v = 0.18140$ ). In addition higher order coefficient have also been estimated from the towing measurements. A pseudo library for lookup table thruster mapping have been created. The bow thruster have been mapped for power limit input =  $\{0.15, 0.3, 0.4, 0.5\}$ , and the voith schneider propellers for speed input =  $\{0.3, 0.4\}$ . Measurments for voith schneider propellers for speed = 0.2 have also been conducted, but no lookup table have been created for it.

The starboard voith schneider propeller rotates slow than the port voith schneider propeller. The effect is notiable in the meaurment. However it does not come into effect unless the maximum force are required, and it becomes less significant as higher rotation speed are used. It is also noted that the servos are significantly coupled and the force output drops at the periphery value , 1 . It can be seen from the thruster measurements that the lookup tables for the voith schneider propellers does not truly cancel out the circular motion of the servos. Some of it can be caused by the rotation when measureing, or due to placement of thuster. However this can not fully explain the notable force measured in the other direction. Of the servos, servo 4 have the strongest coupling in surge-sway.

Two advance control design were implemeted, tuned and tested, a *LgV backstepping* and a *Nonlinear PID* designed controller. In the ideal simulated word both of them were equal in terms of maneuvering. Only ellipse path was used in the laboratory. This had to do with space constraints, and a wish to have long run time on the experiments.

Originally only the *LgV backstepping* was tested in the laboratory. It converged and performed well. The only downside was it would constantly overshoot the heading, resulting in a constant oscillation, while moving along the path. The reason was due to the noisy velocity estimation.

Other opportunity presented itself to run more experiments in the laboratory, However, unknown at that time and discovered too late, one of the servo arms broke due to fatigue from the constant oscillation of the previous runs, corrupting the mapping and observer estimates. In the laboratory, their performance depended heavily on how they were implemented. If both of them were fully implemented, *LgV backstepping* proved to handle the uncertainties better. Although it would overshoot when exiting the sharper part of the ellipse path. The vessel is able to follow the virtual point it is chasing, but the virtual point is unable to stick to the desired path. While the fully implemented *Nonlinear PID* would struggle to converge to the path and behave erratic. The velocity dependent term distorted *Nonlinear PID*'s results the most. The reason is most likely due to the quality of the estimations of the velocities from the observer. The feedforward term also deteriorate the control, and prevents it from converging.

If the *Nonlinear PID* was partially implemented, deactivating the feedforward and the velocity dependent term, then it is the superior one. It would converge naturally to the desired position. Once on, it would stay there indefinitely despite of the broken servo arm.

## 5.1 Future works

With all the improvement in the reliability, one important problem still remains; the loss of visibility.

There are incidents when Qualinsys displays it sees all marks, but it is unable to calculate the vessels position and orientation. The cause of this needs to be further investigated.

Spare part servo arms should be purchased, and padding for the hull to dampen the impact to the basin walls.

Several cracks have been observed on the hull. Simulation Interface Toolkit have been discontinued, modifying it for Modular Interface Toolkit can be an option. The labeling and choice of variable name can be improved upon.

There is a great improvement potential of the contents of this report.

Graphical representation of the simulations and laboratory runs.

Adding comments and details on how the laboratory experiments were conducted.

Editing of the videos taken of the laboratory runs.

Analysis of the hundreds of data measurements taken.

Sorting and organizing the attached files.

Finishing the user manual for **CSE1** and include the complementary screenshots.

# Bibliography

- Breivik, M. and Fossen, T. I. (2005), Principles of guidance-based path following in 2D and 3D, *in* ‘Proceedings of the 44th IEEE Conference on Decision and Control and European Control Conference’, Seville, Spain, pp. 627–634.
- Fossen, T. I. (2002), *Marine Control Systems: Guidance, Navigation, and Control of Ships, Rigs and Underwater Vehicles*, 1st edn, Marine Cybernetics, Trondheim, Norway.
- Fossen, T. I. (2011), *Handbook of Marine Craft Hydrodynamics and Motion Control*, John Wiley & Sons Ltd., United Kingdom.
- National Instruments (n.d.a), ‘Components of a Simulation (Simulation Interface Toolkit)’.  
**URL:** [http://zone.ni.com/reference/en-XX/help/371504F-01/lvsitconcepts/sit\\_c\\_components\\_of\\_a\\_simulation/](http://zone.ni.com/reference/en-XX/help/371504F-01/lvsitconcepts/sit_c_components_of_a_simulation/)
- National Instruments (n.d.b), ‘Understanding the Driver VI (Simulation Interface Toolkit)’.  
**URL:** [http://zone.ni.com/reference/en-XX/help/371504F-01/lvsitconcepts/sit\\_c\\_understanding\\_the\\_driver\\_vi/](http://zone.ni.com/reference/en-XX/help/371504F-01/lvsitconcepts/sit_c_understanding_the_driver_vi/)
- Norwegian University of Science and Technology (n.d.), ‘Marine Cybernetics Laboratory’.  
**URL:** <http://www.ntnu.no/imt/lab/kybernetikk>
- Skåtun, H. N. (2011), Development of a DP system for CS Enterprise I with voith schneider thrusters, Master’s thesis, Norwegian University of Science and Technology.
- Skjetne, R. (2005), The Maneuvering Problem, PhD thesis, Norwegian University of Science and Technology.
- Skjetne, R. (2014), Report: Maneuvering los control design: The fully actuated case. in preparation Rev.E.
- Skjetne, R., Jørgensen, U. and Teel, A. R. (2011), Line-of-sight path-following along regularly parametrized curves solved as a generic maneuvering problem, *in* ‘Proceedings of the 50th IEEE Conference on Decision and Control and European Control Conference’, Orlando, Florida, USA, pp. 2467–2474.
- SNAME (1950), Nomenclature for treating the motion of a submerged body through a fluid, *in* ‘Technical and Research Bulletin No. 1-5’.

Sundland, M. N. (2013), Guidance and control of iceberg towing operation in open water, with experimental testing, Master's thesis, Norwegian University of Science and Technology.

Texas A&M University (n.d.), 'HOW TO CONNECT SIMULINK TO LABVIEW IN ORDER TO COLLECT SYSTEM DATA '.

**URL:** <http://parlos.tamu.edu/MEEN364/Simulink2LabVIEW.pdf>

Thorvaldsen, C. F. L. (2011), Formation control of marine vessels, Master's thesis, Norwegian University of Science and Technology.

Tran, N. D. (2013), Development of a modularized control architecture for cs enterprise i for path-following based on los and maneuvering theory, Technical report.



# Glossary

- .dll** Dynamic-Link Library. [13](#)
- .mdl** MoDeL, file extension. Models created with [Simulink](#). [8](#), [10–14](#), [16](#), [25](#), [40](#)
- .vi** Virtual Instrument, file extension. Basic building block for programs written in [LabVIEW](#). [10–15](#), [39](#)
- B-frame** [CSE1](#)'s body frame. [3](#), [17](#), [21–23](#), [43](#), [44](#)
- Q-frame** [Qualisys](#) inertial reference frame in [MC Lab](#). [3](#), [17–22](#), [43](#), [44](#)
- Base\_Rate\_Loop.vi** Subprogram created by [SIT](#) for input/output of data. [13](#), [14](#)
- Block Diagram** Part of a [.vi](#)-file containing Control Terminals, Wires, Structures and various nodes. The main window used when constructing a [LabVIEW](#) program . [8](#), [10](#), [12–14](#)
- Bluetooth** Wireless technology for exchanging data over short distances. [8](#), [11](#), [39](#)
- BTSix** BlueToothSix, software that enables use of a [Bluetooth PS](#) controller on a computer. [4](#), [8](#), [11](#), [13](#)
- Dongle** Small piece of hardware that attaches to electronic devices enabling additional functions. [8](#), [11](#)
- Front Panel** Part of a [.vi](#)-file containing Controls and Indicators. The main window used when running a [LabVIEW](#) program . [8](#), [10](#), [11](#), [13](#)
- HIL Lab** Hardware In Loop Laboratory, local ethernet in the [MC Lab](#). [8](#), [10](#)
- IO.llb** Program created by [SIT](#) for input/output of data. [14](#)
- LabVIEW** Graphical programming language developed by National Instruments . [4](#), [8](#), [10–16](#), [22](#), [25](#), [39](#)
- MATLAB** Matrix laboratory, high-level technical computing language developed by MathWorks. [4](#), [8](#)
- MCG Reg** Program used for logging data in the [MC Lab](#). [4](#)

- PPJoy** Parallel Port Joystick, software designed to add virtual joysticks under windows operating systems. 4, 8, 11, 13
- Qualisys** Motion capture system. 3, 4, 8–11, 13, 14, 24, 25, 39
- Real-Time Workshop** Generates C/C++ code from **Simulink** diagrams (.mdl-files), rebranded as **Simulink Coder** in later versions. 4, 8, 16, 40
- servo** device used to provide control of a desired operation through the use of feedback. 8, 9
- Simulink** Graphical programming language developed by MathWorks. 4, 8, 13, 15–17, 20, 23–25, 39, 40
- Simulink Coder** Rebranded name of **Real-Time Workshop**. 40
- TeXworks** Program used for writing in LaTeX. 4
- vxworks** Real-time operating system developed as proprietary software by Wind River Systems, designed for use in embedded systems. 13

# Acronyms

**BT** Bow Thruster. 21, 22, 27, 28, 44

**cRIO** Compact Realtime Input and Output. 4, 8, 9, 14, 24, 25

**CSE1** CyberShip Enterprise 1. 1–5, 7–14, 25, 27–31, 39, 46–71

**DOF** Degrees Of Freedom. 4, 18, 20, 21, 43

**DP** Dynamic Positioning. 12, 22

**FPGA** Field-Programmable Gate Array. 4, 10, 14

**GNC** Guidance, Navigation and Control. 4, 24

**GUI** Graphical User Interface. 4, 8, 10–12

**IR** InfraRed. 3, 8–10

**LgV** Control Lyapunov Function. 12

**LgV2** LgV backstepping 2. 5, 22

**LOS** Line-Of-Sight. 2, 18, 20, 21, 43

**MC Lab** Marine Cybernetics Laboratory. 2–5, 7, 8, 10, 11, 39, 40

**MSS** Marine Systems Simulator. 4, 24

**NLPID** Nonlinear **PID**. 5, 22

**PID** Proportional-Integral-Derivative. 1, 5, 22, 41

**PS** PlayStation. 4, 8, 11–13, 22, 39

**QTM** Qualisys Track Manager. 4, 10

**SIT** Simulation Interface Toolkit. 4, 8, 10, 11, 13–15, 24, 39

**VSP** Voith Schneider Propeller. 8, 9, 21, 22, 24, 27, 28, 44



# Symbols

- $\alpha$  Virtual controller. 21, 43
- $\Gamma_q$  Gradient update law tuning matrix. 21, 22
- $\Delta$  Lookahead distance, [m]. 17, 20
- $\eta$  Position and heading in **Q-frame**, vector  $\text{col}(\mathbf{p}, \psi)$ . 3, 21–25, 33
- $\eta_d$  Desired position and heading in **Q-frame**, vector  $\text{col}(\mathbf{p}_d, \psi_d)$ . 33
- $\kappa_1$  Tuning parameter for virtual control  $\alpha$ . 21, 22
- $\lambda$  Gradient update law tuning parameter. 21, 22
- $\mu$  Tuning parameter for  $s$  gradient algorithm. 17, 20
- $\nu$  Velocity in **B-frame**, vector  $\text{col}(u, v, r)$ . 3, 21–25
- $\tau$  Control output,  $\text{col}(X, Y, N)$ . 3, 20, 22–24
- $\chi$  3DOF reference vector in **Q-frame**. 18, 20, 21, 33
- $\psi$  Heading in **Q-frame**, in radians [rad]. 3, 43, 44
- $\psi_d$  Desired heading in **Q-frame**. 19
- $\psi_{los}$  **LOS** heading in **Q-frame**. 18, 21
- $B$  Thruster configuration matrix. 3, 21, 22, 25
- $D$  hydrodynamic damping matrix. 3, 21–25
- $f_{act}$  Thruster force vector,  $\text{col}(f_1, f_2, f_3, f_4, f_5)$ . 3, 4, 22
- $f_q$  Dynamic **LOS** assignment for  $\dot{q}$ . 18, 20, 21
- $f_s$  Dynamic **LOS** assignment for  $\dot{s}$ . 18, 20, 21
- $k$  Scaling parameter of path parameter  $s$ , [-]. 17, 19
- $K_D$  Diagonal tuning matrix. 21, 22
- $K_I$  Diagonal tuning matrix. 21, 22
- $K_P$  Diagonal tuning matrix. 21, 22

- $M$  Inertial matrix. 3, 21–25
- $N$  Moment about z-axis, [Nm]. 43
- $p$  Vessels position as a point mass in  $Q$ -frame, vector  $\text{col}(x,y)$ . 3, 19, 43
- $p_d$  Desired position along desired path in  $Q$ -frame, vector  $\text{col}(x_d,y_d)$ . 17, 18, 22, 44
- $q$  Virtual point-mass coordiantes of vessel in  $Q$ -frame. 17, 18, 20–22
- $r$  Yaw, angular velocity about z-axis in  $B$ -frame, radian per second rad/s]. 3, 43
- $R(\psi)$   $3 \times 3$  rotation matrix between  $Q$ -frame and  $B$ -frame. 3
- $r_x$  Radius of ellipse path in x-direction in  $Q$ -frame, [m]. 17, 19
- $r_y$  Radius of ellipse path in y-direction in  $Q$ -frame, [m]. 17, 19
- $s$  Path parameter of desired path  $p_d$ , [-]. 17–22, 43
- $T_c$  Thruster commands set,  $\text{col}(\mathbf{u}, \text{BT power limit}, \text{VSP speed})$ . 20, 22–24
- $u$  Surge, linear velocity in  $x$ -direction in  $B$ -frame, meter per second [m/s]. 3, 43
- $u_d$  Desired surge speed in  $B$ -frame, [m/s]. 17, 19, 44
- $\mathbf{u}$  Thruster input signals,  $\text{col}(\mathbf{u}_1, \mathbf{u}_2, \mathbf{u}_3, \mathbf{u}_4, \mathbf{u}_5)$ . 4, 22, 44
- $v$  Sway, linear velocity in  $y$ -direction in  $B$ -frame, meter per second [m/s]. 3, 43
- $v_s$  Speed assignment corresponding to  $u_d$ , [m/s]. 19
- $X$  Force in  $x$ -direction, [N]. 43
- $x$  Position in  $Q$ -frame, in meters [m]. 3, 44
- $x_0$  Origin position of ellipse path in  $Q$ -frame, in meters [m]. 17, 19
- $x_1$  Start position of linear path in  $Q$ -frame, in meters [m]. 17, 44
- $x_2$  Direction position relative to  $x_1$  of linear path in  $Q$ -frame, in meters [m]. 17
- $x_d$  Desired position in  $Q$ -frame, in meters [m]. 44
- $Y$  Force in  $y$ -direction, [N]. 43
- $y$  Position in  $Q$ -frame, in meters [m]. 3, 44
- $y_0$  Origin position of ellipse path in  $Q$ -frame, in meters [m]. 17, 19
- $y_1$  Start position of linear path in  $Q$ -frame, in meters [m]. 17, 44
- $y_2$  Direction position relative to  $y_1$  of linear path in  $Q$ -frame in meters [m]. 17
- $y_d$  Desired position in  $Q$ -frame, in meters [m]. 44

## Appendix A

# Thruster plots

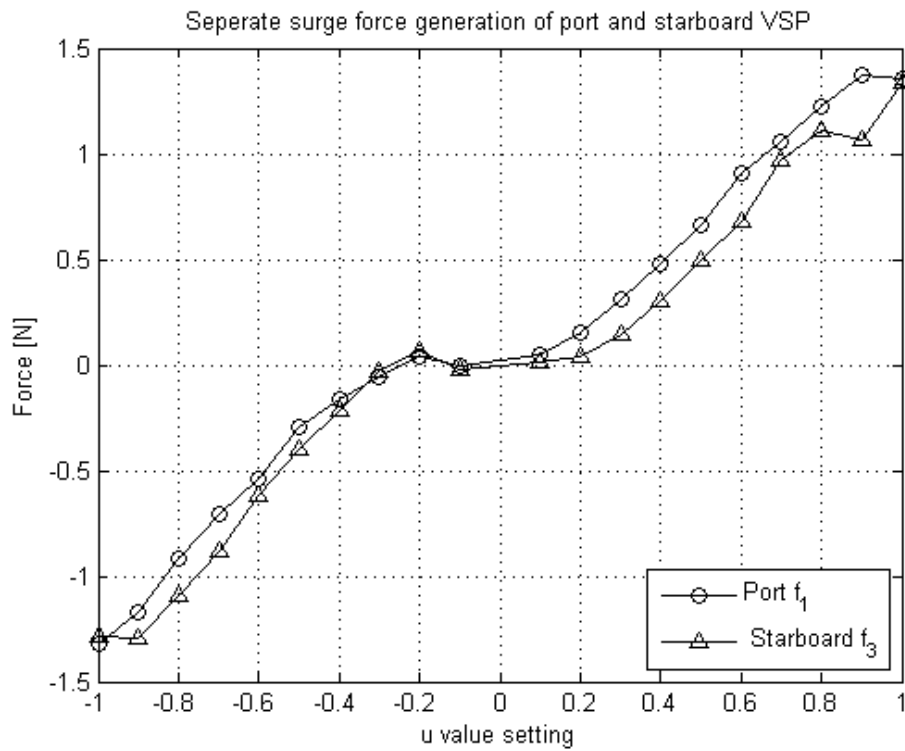


Figure A.1: Measurements of VSP speed at 0.4 coefficient of **CSE1**



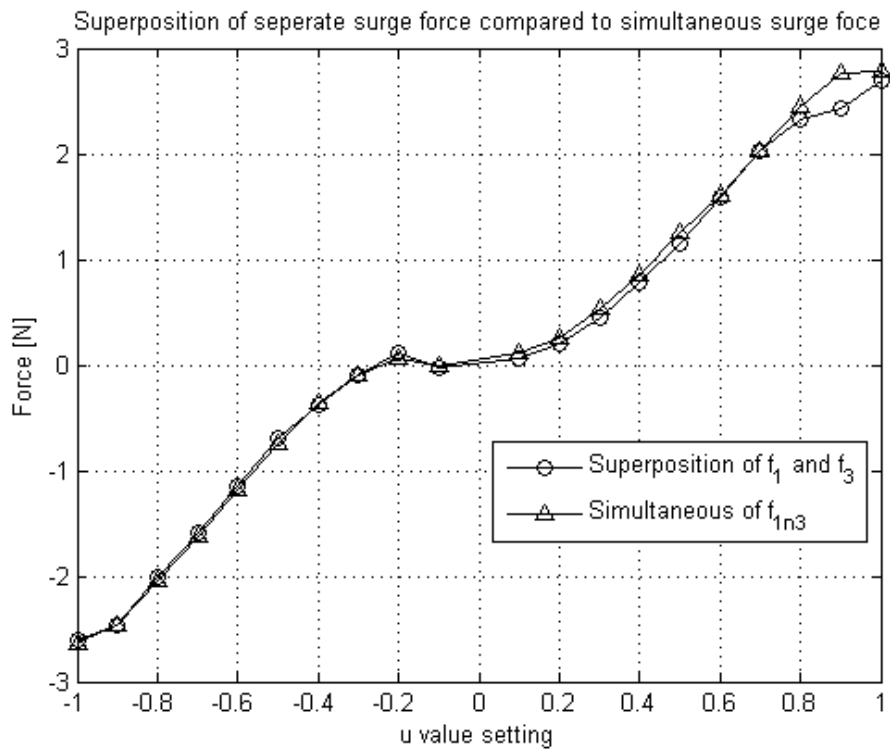


Figure A.2: Measurements of VSP speed at 0.4 coefficient of **CSE1**

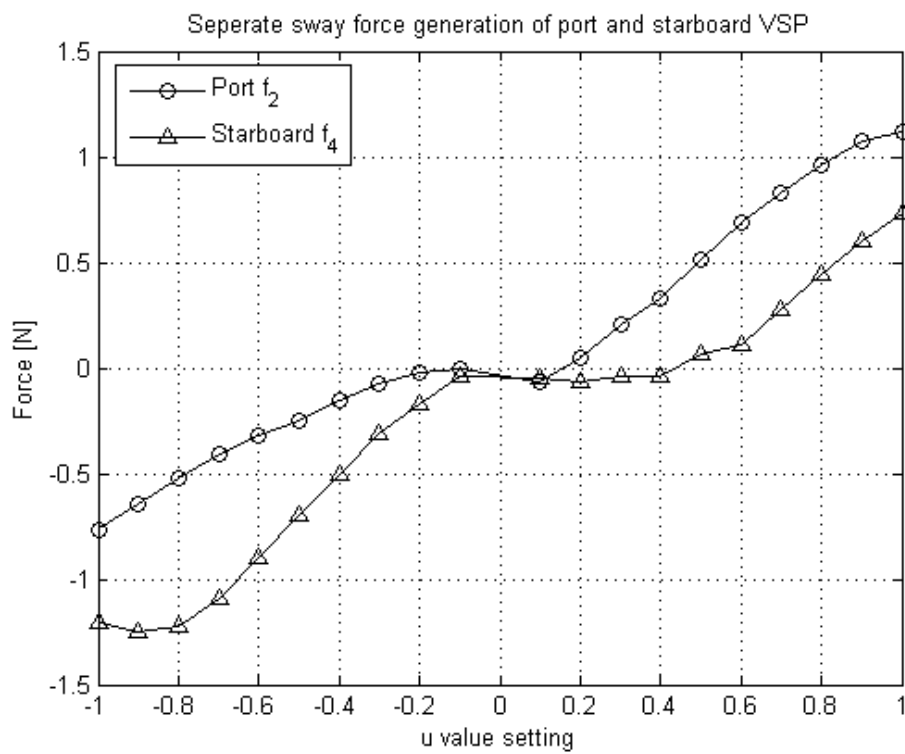


Figure A.3: Measurements of VSP speed at 0.4 coefficient of **CSE1**

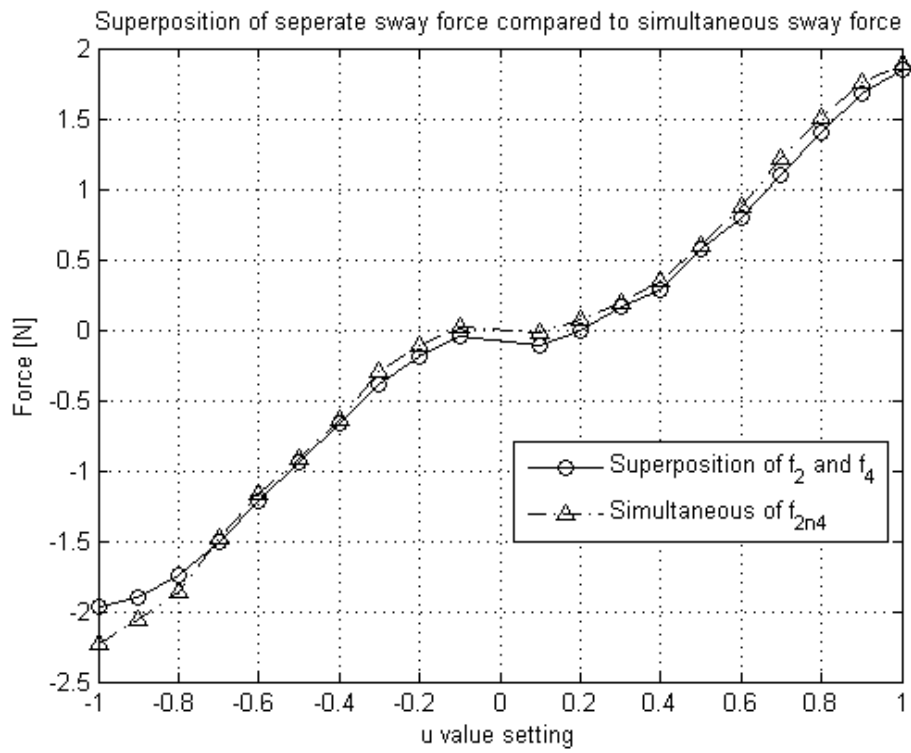


Figure A.4: Measurements of VSP speed at 0.4 coefficient of **CSE1**

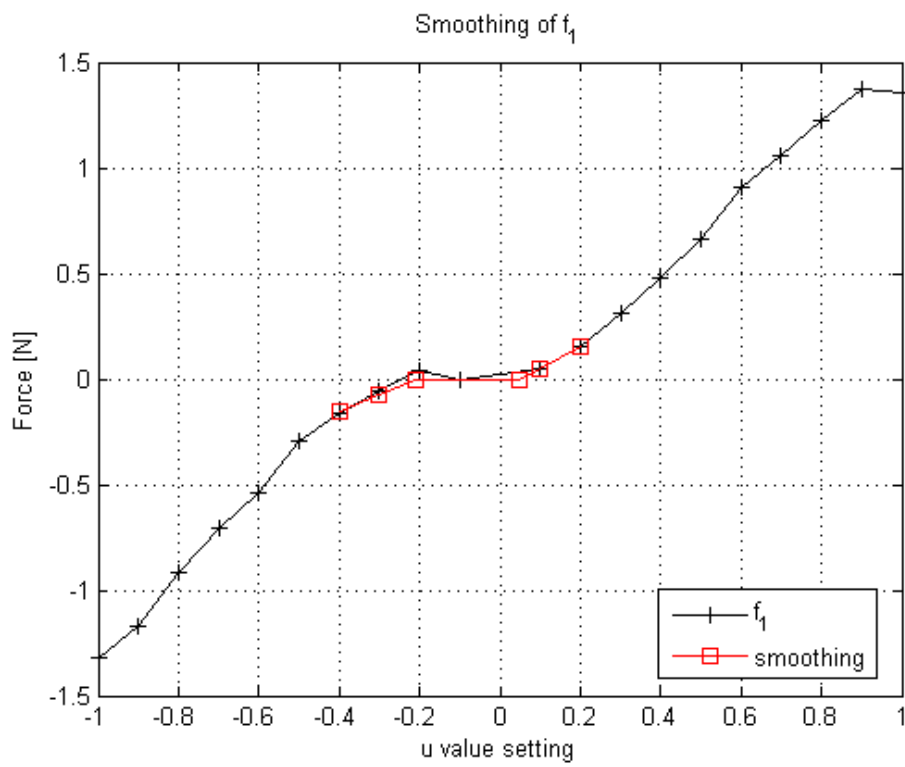


Figure A.5: Measurements of VSP speed at 0.4 coefficient of **CSE1**

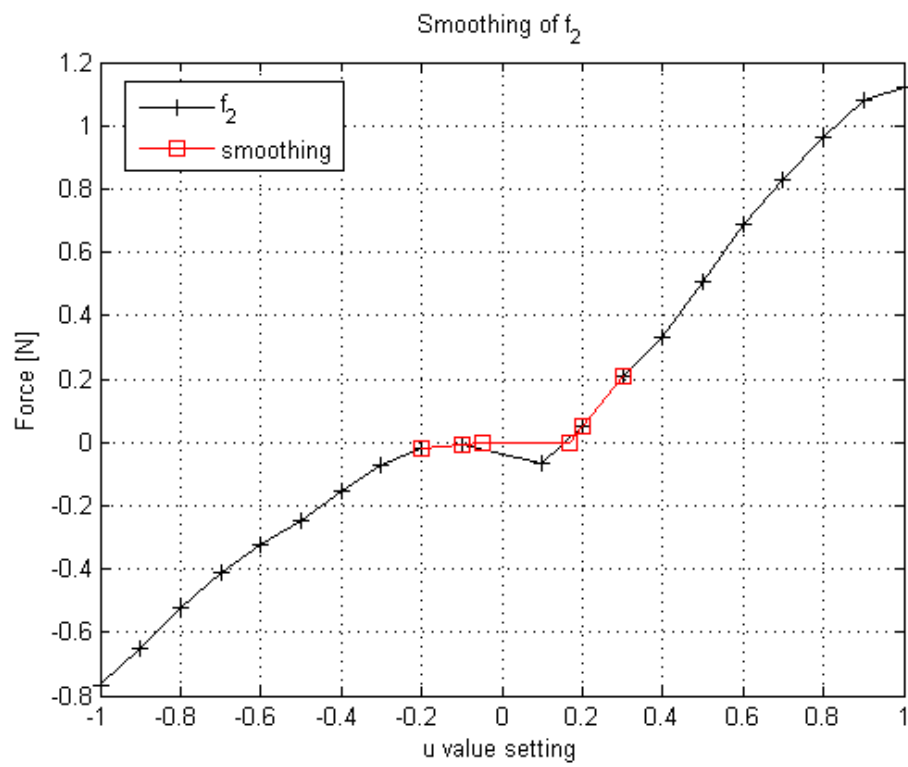


Figure A.6: Measurements of VSP speed at 0.4 coefficient of **CSE1**

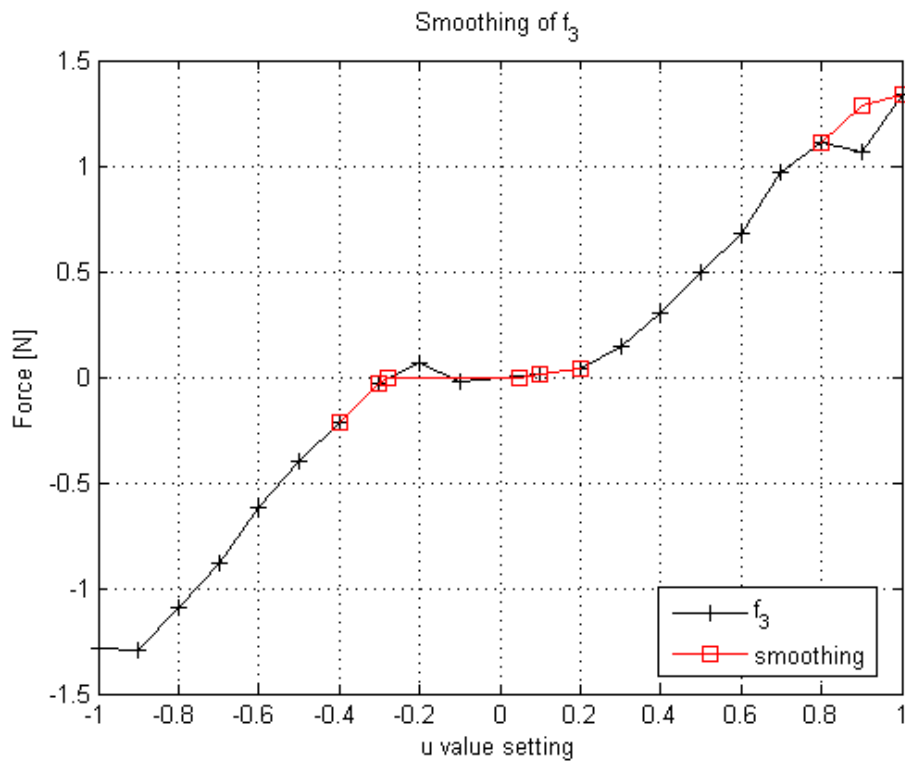


Figure A.7: Measurements of VSP speed at 0.4 coefficient of [CSE1](#)

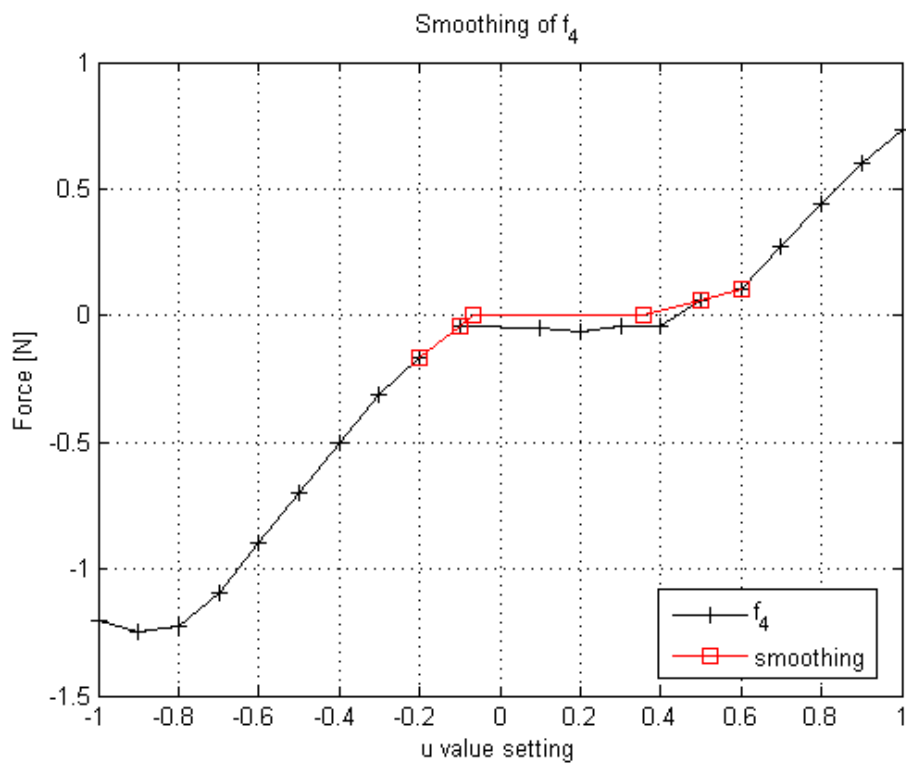


Figure A.8: Measurements of VSP speed at 0.4 coefficient of **CSE1**

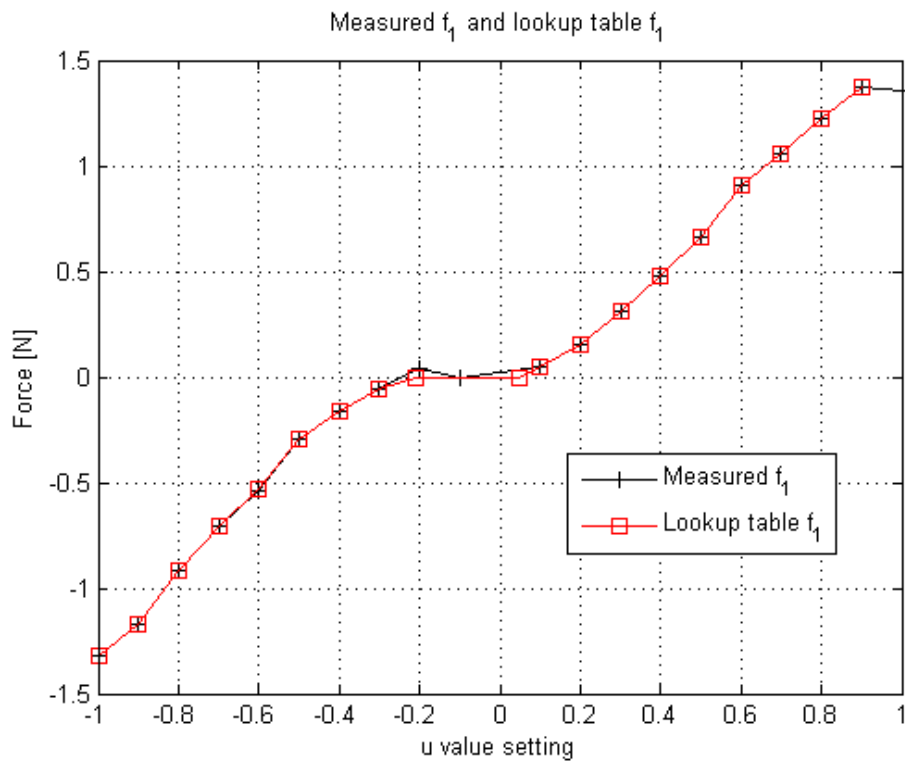


Figure A.9: Measurements of VSP speed at 0.4 coefficient of **CSE1**



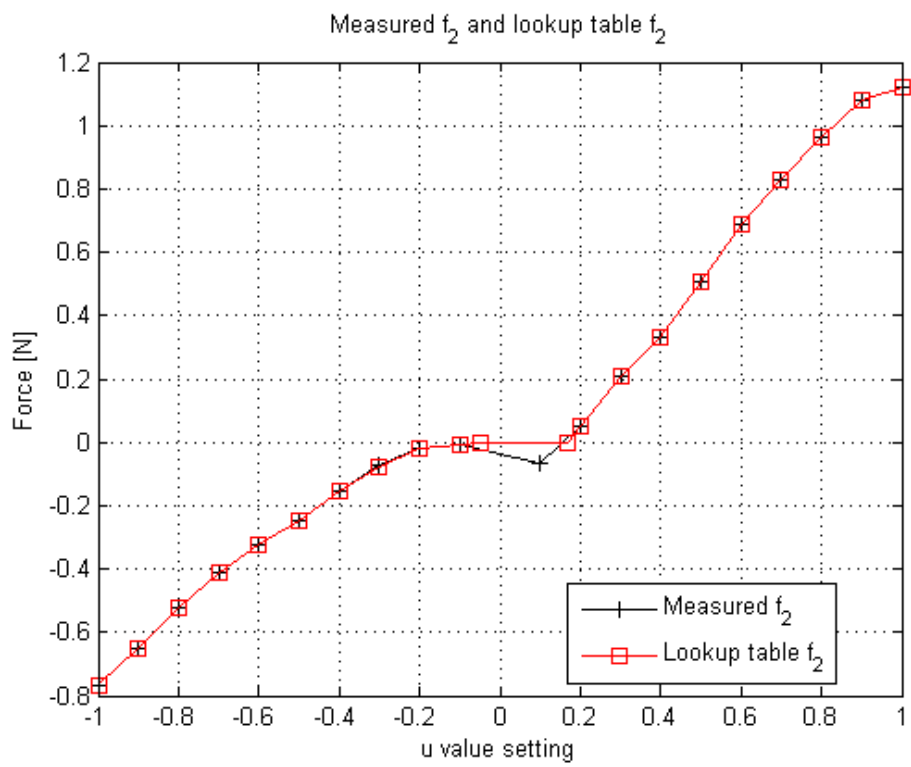


Figure A.10: Measurements of VSP speed at 0.4 coefficient of **CSE1**

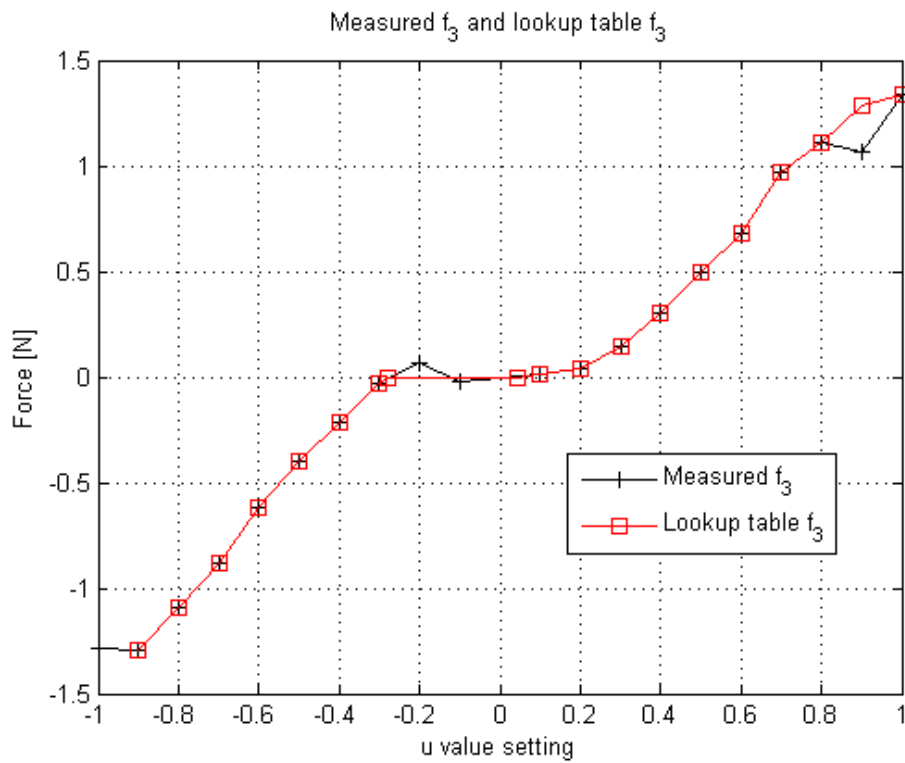


Figure A.11: Measurements of VSP speed at 0.4 coefficient of **CSE1**

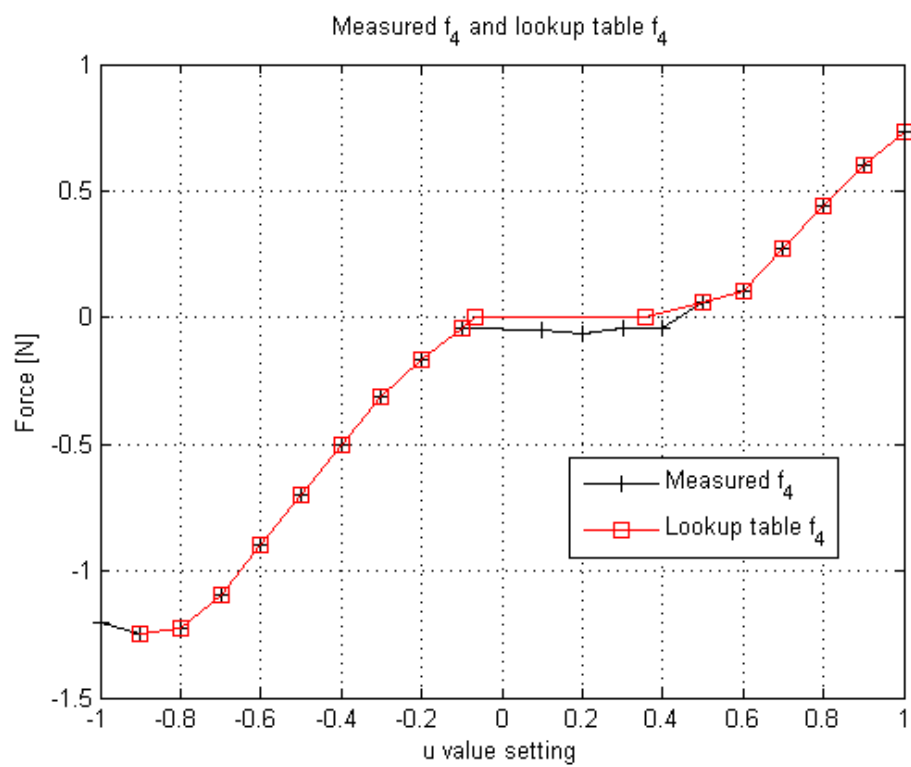


Figure A.12: Measurements of VSP speed at 0.4 coefficient of [CSE1](#)

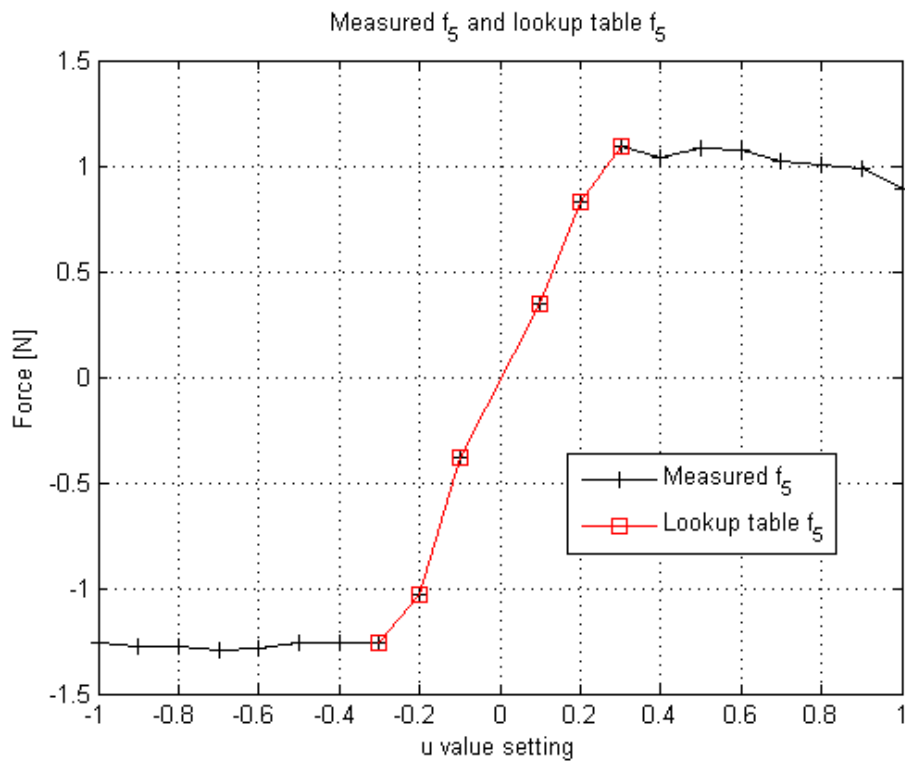


Figure A.13: Measurements of VSP speed at 0.4 coefficient of **CSE1**

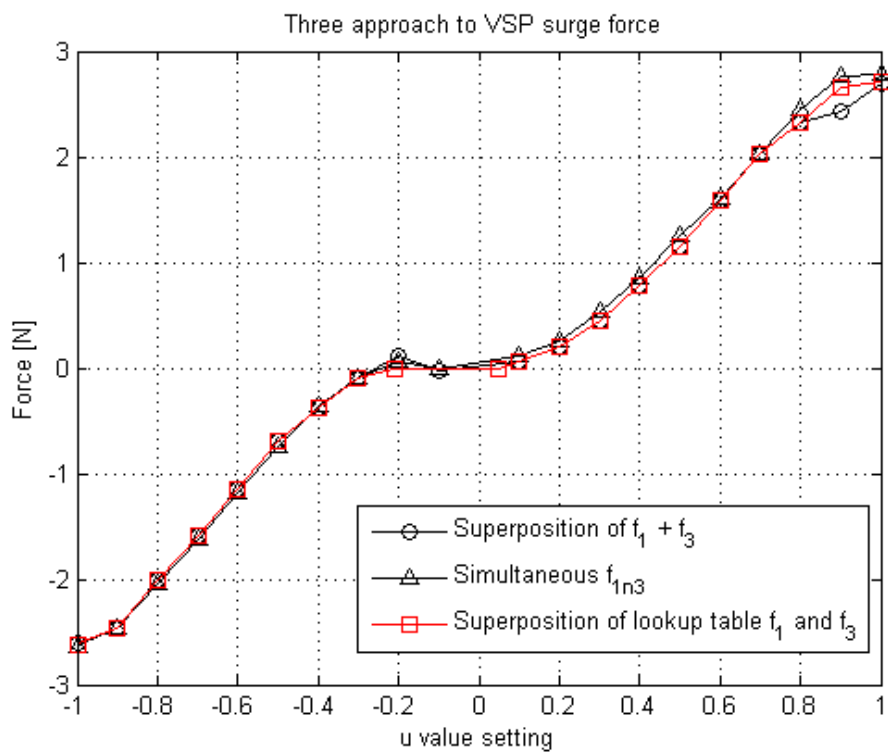


Figure A.14: Measurements of VSP speed at 0.4 coefficient of [CSE1](#)

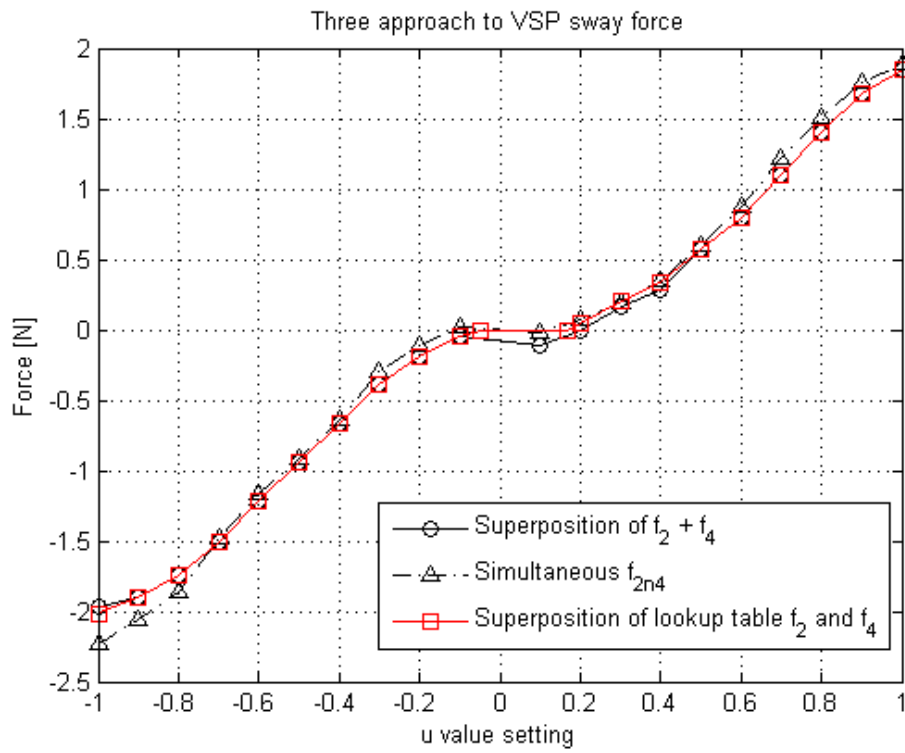


Figure A.15: Measurements of VSP speed at 0.4 coefficient of **CSE1**

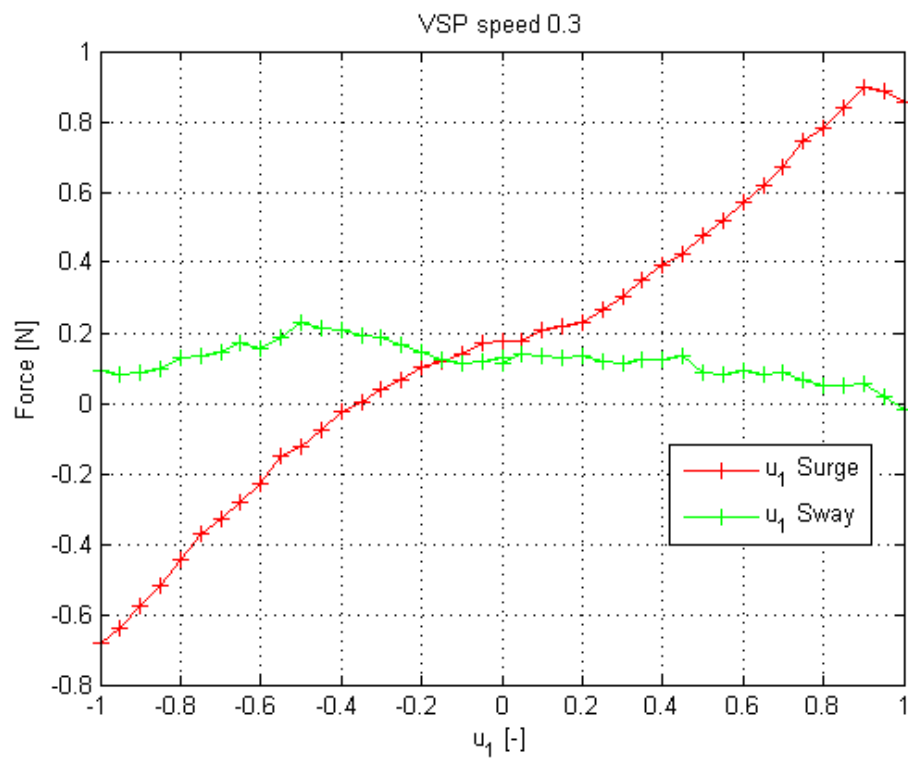


Figure A.16: Measurements of VSP speed at 0.3 coefficient of **CSE1**

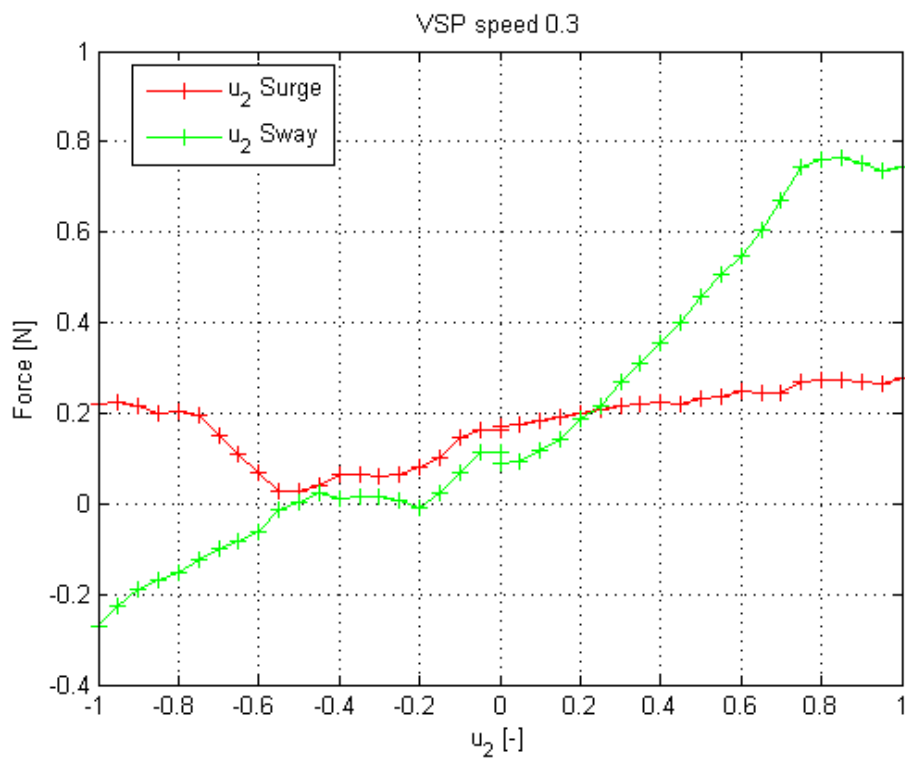


Figure A.17: Measurements of VSP speed at 0.3 coefficient of **CSE1**



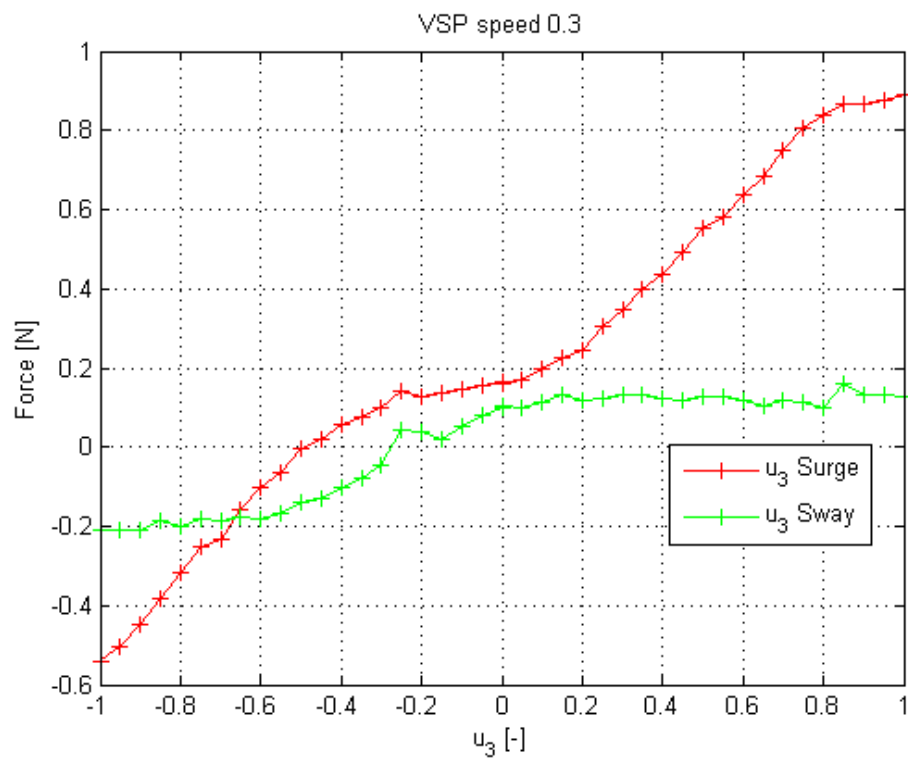


Figure A.18: Measurements of VSP speed at 0.3 coefficient of **CSE1**

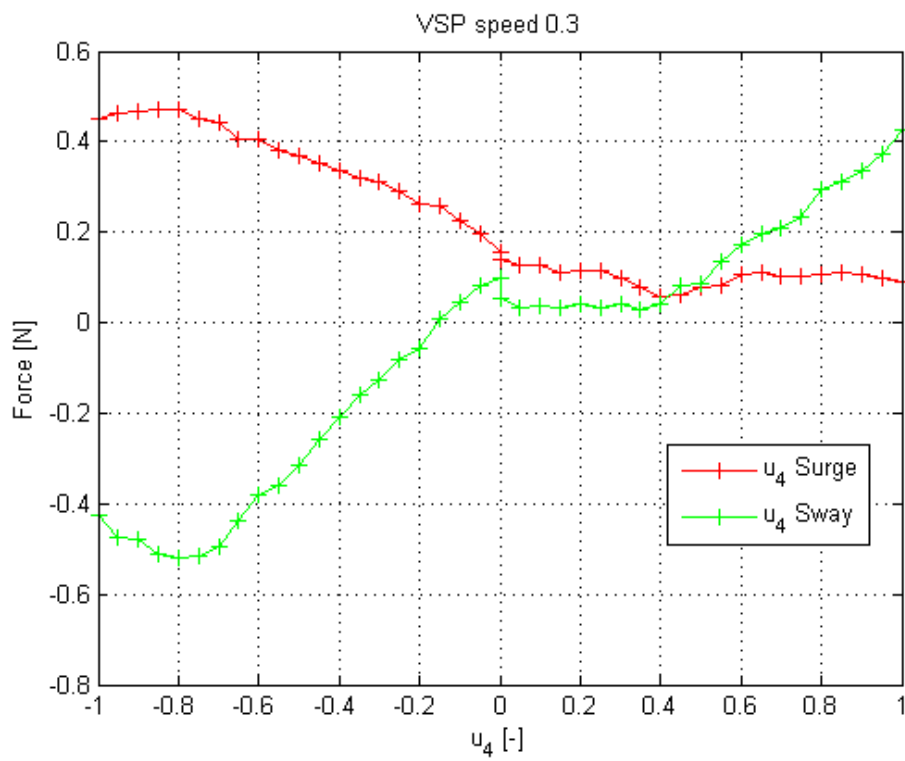


Figure A.19: Measurements of VSP speed at 0.3 coefficient of **CSE1**

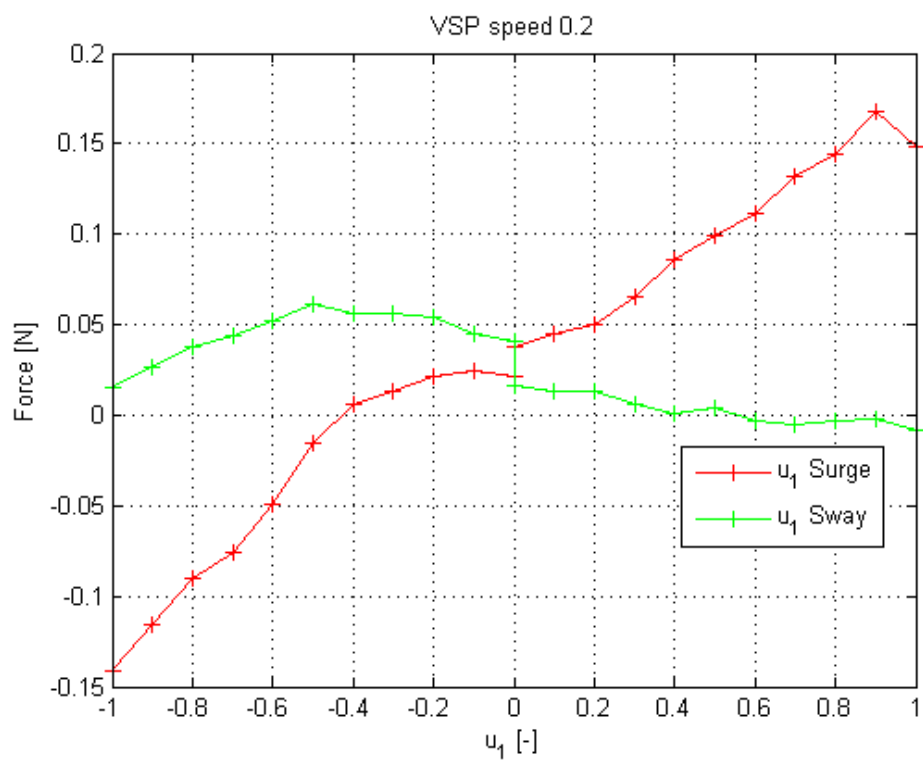


Figure A.20: Measurements of VSP speed at 0.2 coefficient of [CSE1](#)

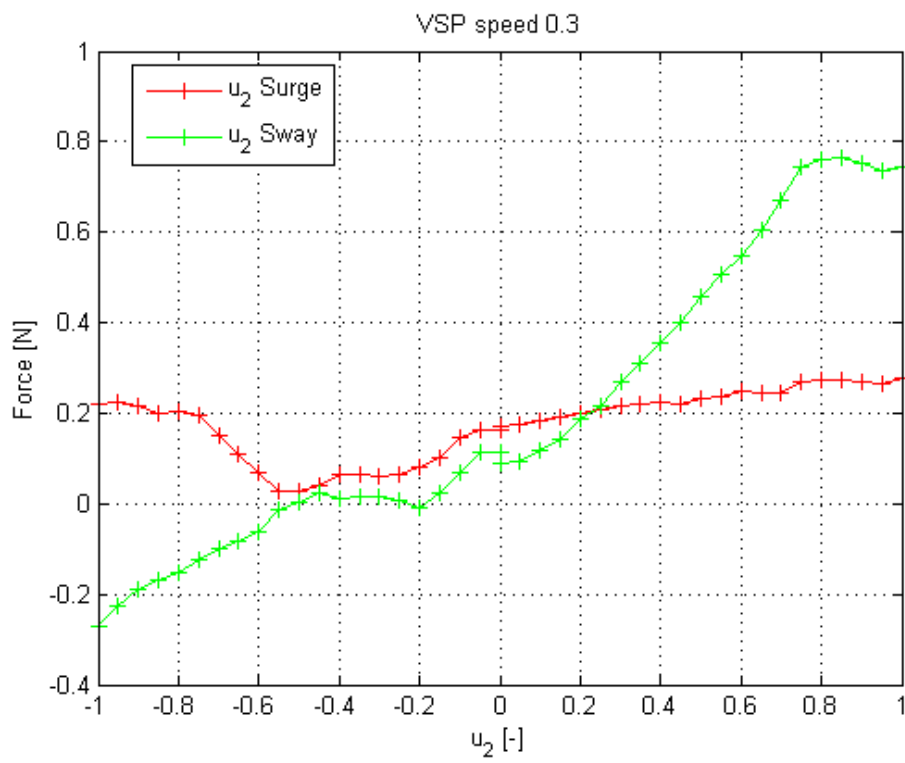


Figure A.21: Measurements of VSP speed at 0.2 coefficient of **CSE1**

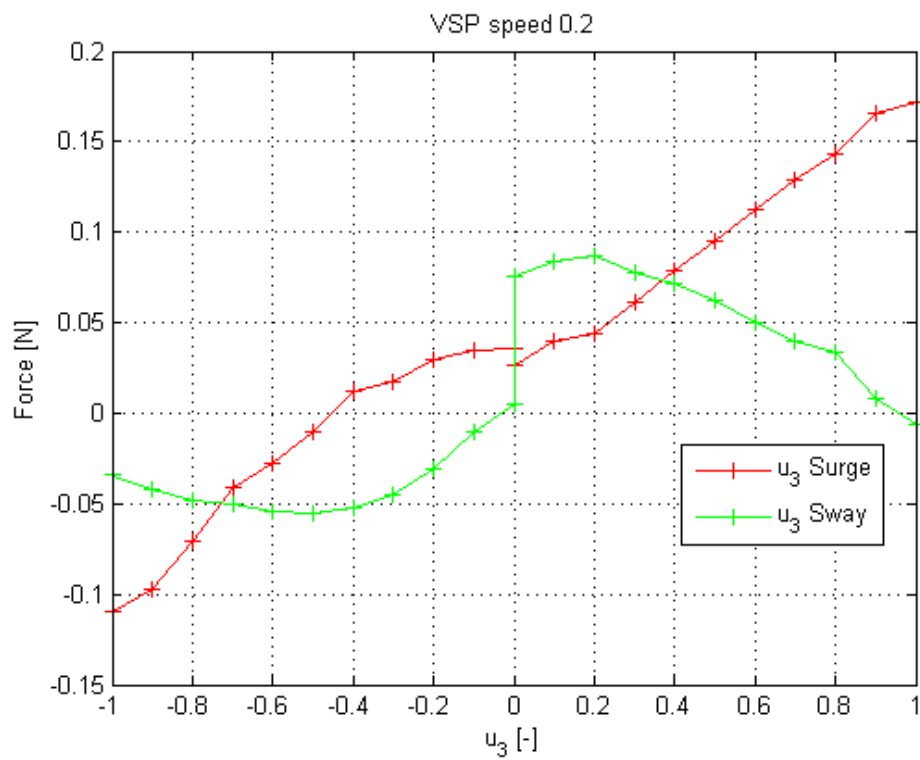


Figure A.22: Measurements of VSP speed at 0.2 coefficient of **CSE1**

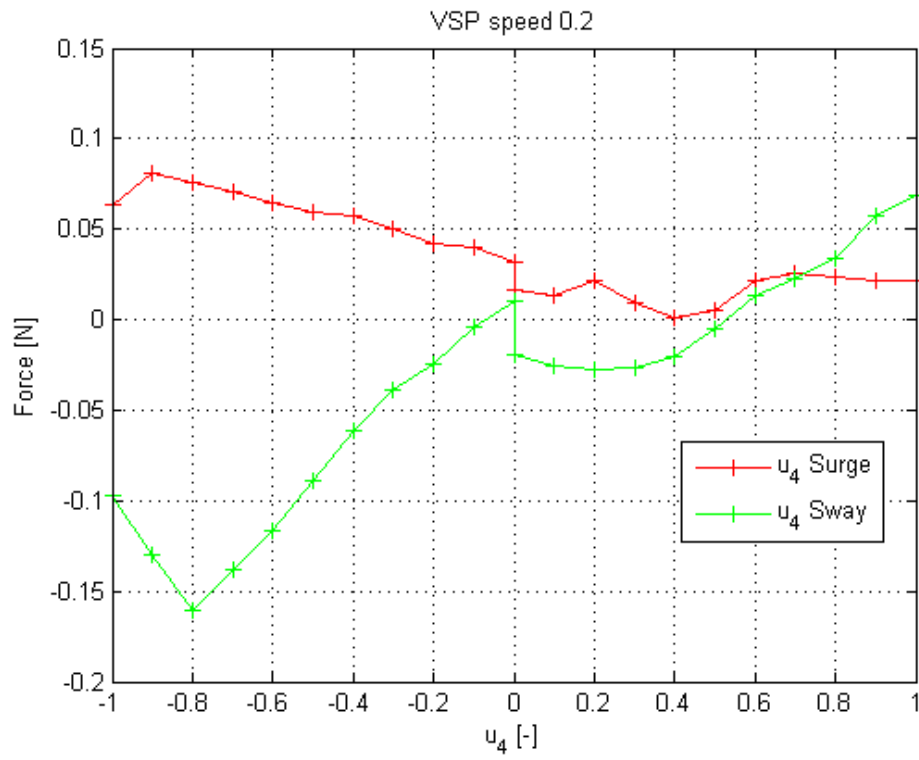


Figure A.23: Measurements of VSP speed at 0.2 coefficient of **CSE1**

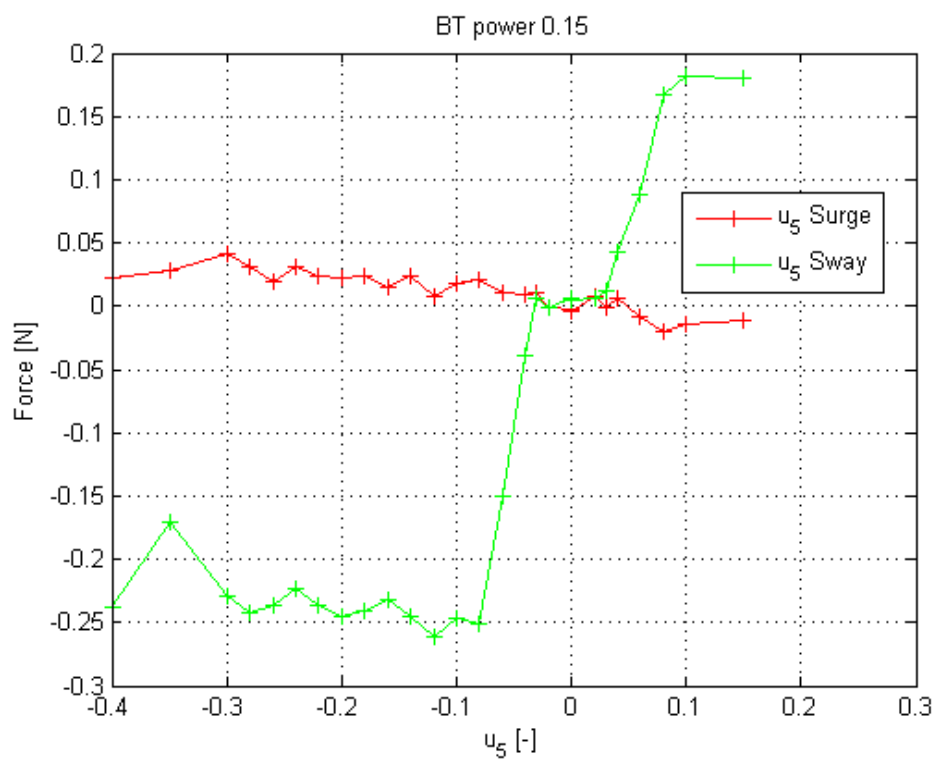


Figure A.24: Measurements of BT power at 0.15 coefficient of [CSE1](#)

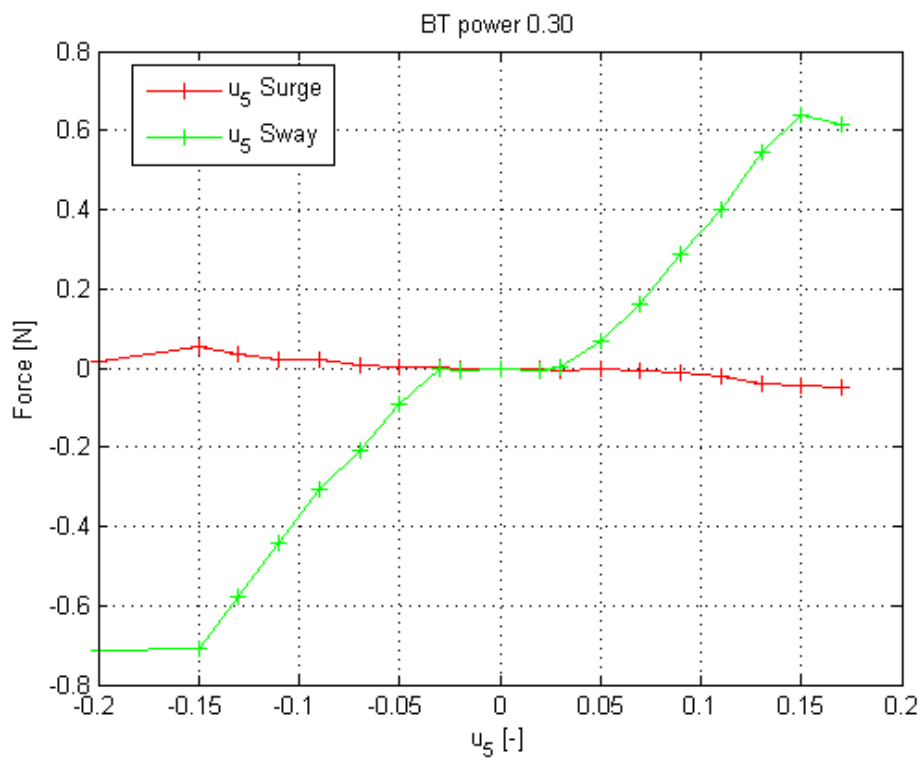


Figure A.25: Measurements of BT power at 0.3 coefficient of **CSE1**



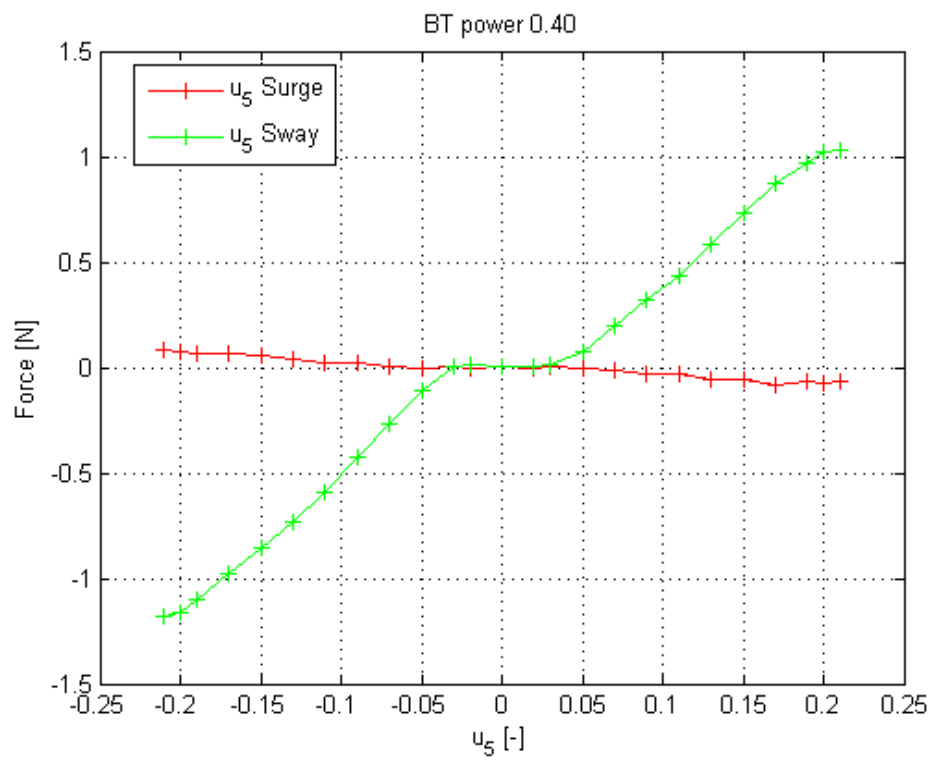


Figure A.26: Measurements of BT power at 0.4 coefficient of **CSE1**



## Appendix B

# Draft for User Manual

Connecting to Cybership Enterprise 1  
(RT CompactRIO - NI-cRIO9024-CSE1 (192.168.0.77))

---

Make sure:

- the ethernet cable is connected to "ACT/LiNK" port 1 and to the "D-Link Wireless Bridge"
- the "Laptop" is connected to "HILLlab"
- the "Main battery" (large fat one) is above 12 Volt
- the "Servo battery" (small slim one) is above 6 Volt

Place "Main battery" (large fat one) beneath wireless antenna, adjacent to waterproof box, between the wires, with battery terminals furthest away from it.

Place "Servo battery" (small slim one) at bow between tunnel thruster and waterproof box, with battery terminals closes to the waterproof box.

Postive battery terminal ("RED-port") at portside and negative battery terminal ("BLACK-port") at starboard side

Connect wire with red isolation ("RED-wire") to "RED-port" and wire with black isolation ("BLACK-wire") to "BLACK-port"

Connect first the "RED-wire" before the "BLACK-wire" to the batteries.

The "Main battery" (large fat one) should be connected first then wait a few sec (5s) before connecting the "Servo battery" (small slim one).

Note: it should not matter in which order it is done, but from experience connecting "RED-wire" before

"BLACK-wire" gives a much higher probability for communication with the CompactRIO on Cybership Enterprise 1 (99-100%'ish) than connecting the "BLACK-wire" before the "RED-wire" (25%'ish), and it is a habit to connect main before the servo, since main powers "CompactRIO" while servo powers "D-Link wireless bridge"

There should be 3 red lights lighting up, one at bow in a purple box for indicating power to tunnel thuster two close to "Main battery", one on each side for each Voith Schneider propeller

The indicators on "ACT/LiNK" port 1 should light up (green) to indicate communication with "HILLlab"

Test communication:

- opening "Command Promt"
- write: ping 192.168.0.77

Command promt should show something like:

```
C:\Documents and Settings\mcl>
```

when opened and

```
C:\Documents and Settings\mcl>ping 102.168.0.77
```

```
Pinging 192.168.0.77: bytes=32 time = 5ms TTL=64
Pinging 192.168.0.77: bytes=32 time = 5ms TTL=64
Pinging 192.168.0.77: bytes=32 time = 5ms TTL=64
Pinging 192.168.0.77: bytes=32 time = 2ms TTL=64
```

Ping statistics for 192.168.0.77:

```
Packets: Sent = 4, Received = 4, Lost = 0 <0% loss>,
Approximate round trip times in milli-seconds:
Minimum =2ms, Maximum = 5ms, Average = 4ms
```

after a successful ping

The most imprtant thing is that you receive packets in return, the time might vary but the important thing is that it responds to the ping.

If Lost = 100% meaning no repons means either "Laptop" or "CompactRIO" is unable to communicate with "HILLlab".

Check Laptop is connected to wireless network "HILLlab", if not connect to it "HILLlab"

Check ACT/LiNK" port 1 are showing activity e.g. are lit, blinking,  
if not check  
ethernet cable is connected to "ACT/LiNK" port 1  
and to the "D-Link Wireless Bridge"  
if not connect to those  
Battery gives power to "CompactRIO" and "D-Link",  
lights/indicators are lit/blinking  
if not check wiring

Check battery voltages,  
"Main battery" should be 10 Volt or more, maximum around  
13 Volt, regular 11 to 12 Volt, low 10 Volt  
"Servo battery" should be in 5 Volt or more, max around  
6.4 Volt, regular around 6 Volt

Note: Black wire should always be the last to be connected,  
and "Main Battery" first

Using PS3 controller

-----  
BtSix.exe need to be running and can be found in the folder :  
...\CS Enterprise I\PS3Control\BtSix.1.5c

BtSix must be active and connected to the PS3 controller prior  
to "Deployment" of the of the vi-file  
Tilting the PS3 controller should give some respons in the  
BtSix window

Make sure the "Joystick info" have under "Device Name";  
"PPJoy Virtual" else the signal might not get through

Scroll to channels untill you get it if it is no the right one

The boolean for the buttons and sticks should light up when  
PS3 controller is used

Avoiding clutter in CS Enterprise I folder:

-----  
Set "Project Directory" in "SIT Connection Manager" as it will  
create five files,  
"...sithwconfig", "...\_Driver.aliases", "...\_Driver.lvproj",  
"...\_Driver.vi and "...\_IO.llb", for each mdl-file "connected"  
with SIT Connection Manager"

Creating nidll.tlc and nidll\_vxworks.tlc files

-----  
 In "Matlab" > "Simulink" > "...mdl"

Set "Current Directory" to "...CS Enterprise I\models\simulink"

Simulation > Configuration Parameters... (Ctrl+E)  
 > Real-Time Workshop >Target selection  
 > System target file: > Browse...

Choose: nidll.tlc > OK >Apply > Build

Then: Brrowse... > nidll\_vxowrks.tlc > OK >Apply > Build

And you have now "...\_nidll\_rtw" and "...\_nidll\_vxworks\_rtw"  
 folder in "...CS Enterprise I\models\simulink" where "..."  
 is the name of the mdl-file. e.g.  
 StudentTemplate.mdl gives StudentTemplate\_rtw and  
 StudentTemplate\_nidll\_vxworks\_rtw

Connecting vi-file to mdl-file, Real-Time Target  
 -----

1. In "Matlab" "Simulink": create using RealTime Workshop,  
nidll.tlc and nidll\_vxworks.tlc files for the desired mdl-file
2. Make sure you are able to communicate with the  
cRIO on C/S Enterprise 1  
- Check by "Command Promt" > ping 192.168.0.77)
3. Open SIT Connection Manager  
- "...vi" > "Front Panel" > "Tools" > "SIT Connection Manager ..."
4. In "Execution Host", have the "Real-Time Target" selected  
- "Target" is "RT CompactRIO - NI-cRIO9024-CSE1 (192.168.0.77)"
5. "Add Targets and Devices on ...\_Driver.lvproj"  
> "Targets and Devices" > "Real-Time CompactRIO" folder  
> " NI-cRIO9024-CSE1"
6. "Select Programming Mode" > "LabVIEW FPGA Interface"
7. "Current Model DLL", select the dll-file created in step 1 inside the folder  
"...\_nidll\_rtw"  
- the dll-file should have the same name as the mdl-file it was created from
8. Change "Project Directory" to "...\CS EnterpriseI\Project folder  
You might have to redo step 5 again

=====

Starting from a clean slate hardware mapping in "SIT Connection Manager ...":

1. "Hardware I/O" > "Configure HW I/O..."
2. Easiest with "Import..." and select the hardwaremapping file or Right click on "Device Tree" on the IP address: 192.168.0.77
- 3: Select Add Device > NI-FPGA
- 4: In "NI-FPGA Property Dialog"
  - The "FPGA Target" should be:
  - most often something ending with "... - cRIO-9113"
  - The "FPGA Bitfile" should be the appropriate file:  
if only input signals from battery voltages and Qualisys:  
"sitfpga cRIO-9113 IO CSE.lvbitx" authored by  
Senior Engineer Torgeir Wahl  
if with forcing: "sitfpga cRIO-9113 IO CSE Strain.lvbitx"  
authored by Senior Engineer Torgeir Wahl
  - In "Options" all "PWM out..." Frequency should be set to 50 Hz,  
else strange behavior/ damage may happen

Sometimes when deploying, a "Conflict Resolution" window may pop up, this means there is already a previous vi-file already deployed and may also be running on the cRIO

press "Apply" will override the old stuff from a previous run

If unable to resolve the conflict, restart the cRIO by

1. Use "Measurement & Automation" (program found on desktop) and remotly restart cRIO, if that fails
2. Disconnect and reconnect all power sources (batteries)

=====

Qualisys:

Qualisys Oqus: The cameras used to register/see the IR markers

Qualisys Motion Capture Systems: is the system that process the data from Oqus

Qualisys Track Manager: The userinterface to interact with Motion Capture System

=====

QTMdriver.vi

The QTMdriver is engineered by Senior Engineer Torgeir Wahl to aquire the data from Qualisys.

It is:

- built in a producer-consumer pattern, this decouples the capture-rate of Qualisys and the mdl solver-rate
- built to handle any number of bodies Qualisys needs to track
- 0-index based and passes the signals in the following order:
  1. Frame number
  2. Error signal

3. x-position in millimeter 1.body
  4. y-position in millimeter 1.body
  5. z-position in millimeter 1.body
  6. yaw in degrees 1.body
  7. pitch in degrees 1.body
  8. roll in degrees 1.body
  9. Residual, mean offset between all the IR markers compared to the expected position-configuration 1.body
  10. x-position in millimeter 2.body
  11. y-position in millimeter 2.body
  12. z-position in millimeter 2.body
  13. yaw in degrees 2.body
  14. pitch in degrees 2.body
  15. roll in degrees 2.body
  16. Residual, mean offset between all the IR markers compared to the expected position-configuration 2.body
- etc.

The driver will send only the lastet/newest data

- queues up all data given from Qualisys and send the newest dataset when data is requested
  - after sending the latest dataset it will purge the queue, but hold on the the latest dataset
  - if capture rate is higher/faster than solver rate then, no all data recieved from Qualisys will be used
  - if capture rate is lower/slower than solver rate then, same data will be sent one or several times untill new data is available
- e.g will act as a zero order hold model

For one body tracking use: QTMDriver\_OneBody.vi

For two body tracking use: QTMDriver\_TwoBodies.vi

For three or more body tracking:

1. Make a copy of QTMDriver\_OneBody.vi or QTMDriver\_TwoBodies.vi in the same folder
2. Rename it to an appropriate name e.g. for tracking three bodies QTMDriver\_ThreeBodies.vi
3. Open it and go to "Block diagram"
4. Inside "While Loop" go to "Case Structure"> Case "Read"
5. In there is another "Case Structure", To the right of it is a "Array Subset" with 2 constant block attached to it.  
One of those is "0" to indicate first index, the other one is "2+(number of bodies)\*7". input the correct number in the second one



that determines the length of the array. e.g. one body == 9, two bodies == 16, 3 bodies == 23 etc.

6. exit and save.

7. NB the "SIT input block" in Simulink mdl-file should have the same port size as the length of the array specified in the QTMdriver, else it may spill over onto other sit input ports or become suffled in the order they are sent

=====

Acquiring QTM data: Connect QTMdriver to .vi

The data from Qualisys is never explicitly mapped anywhere, but it is handled by the FPGA file selected in the hardware mapping e.g.

"sitfpga cRIO-9113 IO CSE.lvbitx"

After Connecting the LabVIEW vi-file (TemplateLV\_HMI.vi) to the mdl-file (TemplateSL.mdl) via the dll-file (TemplateSL.dll) created

through Realtime Workshop in Simulink using SIT Connection Manager in the vi-file (TemplateLV\_HMI.vi),

see previous note on connecting .vi to .mdl.

The SIT Connection Manager should have created several files in the chosen designated "Project Directory" with filenames begining with the mdlfilename.

e.g. "TemplateSL.mdl" will produce:

TemplateSL.sithwconfig

TemplateSL\_Driver.aliases

TemplateSL\_Driver.lvproj

TemplateSL\_Driver.vi

TemplateSL\_IO.llb

- Open the input-output-library e.g. "TemplateSL\_IO.llb"
- Open baserate loop.vi e.g. "TemplateSL\_Base Rate Loop.vi"
- From "Front Panel" go to "Blockdiagram, "Ctrl+E" or "Windows>Show Block Diagram"
- Add the QTM driver inside "Init Code"-, "Read Code"- and "Close Code"-Flat Sequence Structure (Gray frames below the name tags)
- NB do not add the QTM driver to the "Write Code"-Flat Sequence Structure)
- Add QTM driver by (inside the Block Diagram):
  1. "right click" to get "function curtain
  2. Click on "Select a VI..."
  3. Go to "QTMdrivers" folder, and select appropriate driver. e.g. "QTMdriver\_OneBody.vi
- Tip. add one as decribed above and select the added block, hold "Ctrl" and drag it to copy it
- Connect the vi's together

Tip 1: Have "Context Help" window open

Tip 2: "right click" on the vi-block and uncheck "View as Icon

Tip 3: "Ctrl+U" or "Edit"> "Clean Up Diagram" will automatically organize the wire and blocks for you, if you dont like it press "Ctrl+z" or "Edit">"Undo Window Move" to undo it

0. ONLY delete all wires inside "Init Code"-, "Read Code"- and "Close Code"-Flat Sequence Structure (Gray frames below the name tags)

1. Hover above "Ring" port (blue top left) > "right click" > "Create" > "Constant"

2. Repeat 1. for all added vi-blocks

3. For each constant change it to appropriate "Value", by "left click" "Constant" and select correct "value"

- For vi-block in "Init Code Flat Sequence Structure": "Constant" == "Init"
- For vi-block in "Read Code Flat Sequence Structure": "Constant" == "Read"
- For vi-block in "Close Code Flat Sequence Structure": "Constant" == "Close"

4. For all Flat Sequence Structure with vi-blocks, connect "Error wire"(alternating yellow/black wire) to it,

- left "Error" port to "error in" port
- "error out" port to right "Error" port

5. From "Init Code"Flat Sequence Structure vi-block port to "Read Code" Flat Sequence Structure vi-block port

- "Connection ID out" to "Connection ID" (Turquoise wire )
- "QTMqueue Out" to "QTMqueue" (Orange with turquoise shell wire )
- "VI Refnumb QTMTTask Out" to "VI Refnumb QTMTTask" (light turquoise wire)

6. "Read Code" Flat Sequence Structure vi-block

- Hover above "DataOutIndex" port "right click"
- > "Create" > "Constant" and set "Constant" == 0
- Connect Flat Sequence Structure "presized input array" (Orange wire) port to vi-block
- left "presized input array" port to "DataIn" port
- "DataOut" port to right "presized input array" port

7. From "Read Code"Flat Sequence Structure vi-block port to "Close Code" Flat Sequence Structure vi-block port

- "Connection ID out" to "Connection ID" (Turquoise wire )
- "QTMqueue Out" to "QTMqueue" (Orange with turquoise shell wire )
- "VI Refnumb QTMTTask Out" to "VI Refnumb QTMTTask" (light turquoise wire)

8. Save and exit